SUPPORTING INFORMATION

Photocontrol of Anion Binding Affinity to a Bis-Urea Receptor Derived from Stiff-Stilbene

Sander J. Wezenberg,* and Ben L. Feringa

Stratingh Institute for Chemistry, University of Groningen,
Nijenborgh 4, 9747 AG, Groningen, The Netherlands

Email: s.j.wezenberg@rug.nl

Table of contents

Experimental Section S2

^{1}H and ^{13}C NMR Spectra of new compounds S5

^{1}H NMR photoisomerization studies S16

Quantum yield determination S17

^{1}H NMR titration experiments S18

Job plot and titration curve analysis S27

Geometry optimizations by DFT S32

References S37

Experimental Section

General methods and materials:

THF, toluene and CH_2Cl_2 were dried by using an MBraun solvent purification system. Dry DMSO and DMSO-d_6 were purchased from Acros Organics and were stored under N_2 over molecular sieves (4Å). The degassing of solvents was carried out by purging with N_2 for 30 min. All other chemicals were commercial products and were used as received. Flash chromatography (FC) was performed using silica gel (SiO_2) purchased from Merck (type 9385, 230-400 mesh) and thin-layer chromatography (TLC) was carried out on aluminum sheets coated with silica 60 F254 obtained from Merck; compounds were visualized with a UV lamp (254 nm) or by staining with phosphomolybdic acid (PMA). Melting points (m.p.) were determined using a Büchi-B545 capillary melting point apparatus. ^{1}H and ^{13}C spectra were recorded on Varian Mercury-Plus 400 and Varian Mercury-Plus 600 spectrometers at 298K unless indicated otherwise. Chemical shifts (δ) are denoted in parts per million (ppm) relative to DMSO-d_6 (for ^{1}H detection, δ = 2.50 ppm; for ^{13}C detection, δ = 39.52 ppm). Due to poor solubility, DMSO and H_2O peaks in the NMR spectra are larger than the compound peaks. The splitting pattern of peaks is designated as follows: s (singlet), d (doublet), t (triplet), (multiplet), br (broad), or dd (doublet of doublets). High-resolution mass spectrometry (ESI-MS) was performed on a LTQ Orbitrap XL spectrometer with ESI ionization. UV-vis spectra were recorded on Specord S600 and Hewlet-Packard HP 8543 diode arrays, equipped with a Quantum Northwest Peltier controller, in a 1 cm or 1 mm quartz cuvette. Irradiation of UV-vis samples was carried out at 20 °C using a Thorlab model M365F1 high-power LED (4.1 mW) and a Thorlab model M385F1 high-power LED (10.7 mW) positioned at a distance of 1 cm. NMR irradiation studies were performed at 20 °C with a Thorlab model M365FP1 high-power LED (15.5 mW) and a Thorlab model M385FP1 high-power LED (23.2 mW) coupled to a 600 μm optical fiber, which guided the light into the NMR tube inside the spectrometer.[1]

(*E*)/(*Z*)-6,6'-dibromo-2,2',3,3'-tetrahydro-1,1'-biindenylidene [(*E*)/(*Z*)-2]:

Titanium(IV) chloride (3.30 mL, 30.0 mmol) was slowly added to zinc powder (3.93 g, 60.0 mmol) in THF (30 mL) under a N_2 atmosphere and under vigorous stirring. The solution was stirred at reflux for 2 h and cooled back to rt, after which solid 6-bromo-1-indanone (3.17 g, 15.0 mmol) was added to the black suspension. The mixture was stirred at reflux for a further 24 h, treated with a saturated aqueous NH_4Cl solution, and extracted with $CHCl_3$ (3 × 100

mL). The volume of the combined extracts was reduced to 30 mL and the precipitate was filtered off and air-dried to afford (*E*)-**2** (842 mg, 29%) as an off-white solid; m.p. 240.7 – 242.6 °C; ^{1}H NMR (400 MHz, DMSO-d_6, (*E*)-geometry assignment based on a NOESY spectrum): 7.68 (d, *J* = 1.8 Hz, 2H; 2 arom. H), 7.42 (dd, *J* = 8.0, 1.7 Hz, 2H; 2 arom. H), 7.33 (d, *J* = 8.0 Hz, 2H; 2 arom. H), 3.14-3.02 (m, br. 8H; 4 CH_2); too insoluble for a ^{13}C NMR measurement. The filtrate was concentrated and FC (SiO_2, pentane) afforded (*Z*)-**2** (673 mg, 23%) as a white solid; m.p. 137.6 – 139.9 °C; ^{1}H NMR (400 MHz, DMSO-d_6): 8.01 (s, 2H; 2 arom. H), 7.40 (d, *J* = 8.0, 2H; 2 arom. H), 7.32 (d, *J* = 8.2 Hz, 2H; 2 arom. H), 2.95-2.89 (m, br. 4H; 2 CH_2), 2.92-2.75 (m, br. 4H; 2 CH_2); ^{13}C NMR (100 MHz, DMSO-d_6): 147.6, 141.8, 135.1, 130.1, 127.5, 125.0, 118.7, 34.4, 29.6.

(*E*)-2,2',3,3'-tetrahydro-(1,1'-biindenylidene)-6,6'-diamine [(*E*)-3]:

Compound (*E*)-**2** (960 mg, 2.46 mmol), palladium(II) acetate (44 mg, 0.20 mmol), DPPF (136 mg, 0.25 mmol) and sodium tert-butoxide (473 mg, 4.92 mmol) were brought under a N_2 atmosphere in a Schlenk tube via three vacuum/N_2 cycles. Then degassed toluene (12 mL) was added, followed by benzophenone imine (1.03 mL, 6.15 mmol). The mixture was stirred at 90 °C for 20 h, cooled to rt and diluted with water (10 mL). The aqueous layer was extracted with $CHCl_3$ (3 × 25 mL) and the combined organic phases were dried over Na_2SO_4 and concentrated. FC (SiO_2, 0.1% NEt_3 in CH_2Cl_2) afforded the imine intermediate as a yellow solid, which was redissolved in THF (100 mL). A 2M aqueous HCl solution (50 mL) was added and after 1.5 h of stirring, the solution was made basic by addition of a saturated aqueous $KHCO_3$ solution (pH ~ 10). The mixture was extracted with EtOAc (3× 50 mL) and the combined organic phases were dried over Na_2SO_4 and concentrated. The product was precipitated in Et_2O, filtered off and air-dried to afford (*E*)-**3** (503 mg, 78%) as a light-brown solid; m.p. 260 °C (decomp); ^{1}H NMR (400 MHz, DMSO-d_6): 6.97 (d, *J* = 8.0 Hz, 2H; 2 arom. H), 6.87 (d, *J* = 2.0 Hz, 2H; 2 arom. H), 6.45 (dd, *J* = 8.0, 1.9 Hz, 2H; 2 arom. H), 4.89 (s, 4H; 2 NH_2), 3.03-2.84 (m, br. 8H; 4 CH_2); ^{13}C NMR (100 MHz, DMSO-d_6): 147.2, 143.4, 134.7, 134.1, 124.7, 113.6, 109.8, 31.9, 29.5; HRMS (ESI) *m/z*: 263.1544 ($[M+H]^+$, calcd for $C_{18}H_{19}N_2^+$: 263.1543).

(*Z*)-2,2',3,3'-tetrahydro-(1,1'-biindenylidene)-6,6'-diamine [(*Z*)-3]:

Compound (*Z*)-**2** (735 mg, 1.88 mmol), palladium(II) acetate (34 mg, 0.15 mmol), DPPF (104 mg, 0.19 mmol) and sodium tert-butoxide (362 mg, 3.77 mmol) were brought under a N_2 atmosphere in a Schlenk tube via three vacuum/N_2 cycles. Then degassed toluene (9 mL) was added, followed by benzophenone imine (0.79 mL, 4.71 mmol). The mixture was stirred at 90

°C for 16 h, cooled to rt and diluted with water (10 mL). The aqueous layer was extracted with CH_2Cl_2 (3 × 25 mL) and the combined organic phases were dried over Na_2SO_4 and concentrated. FC (SiO_2, 0.1% NEt_3 in CH_2Cl_2) afforded the imine intermediate as a yellow oil, which was redissolved in THF (20 mL). A 2M aqueous HCl solution (10 mL) was added and after 30 min of stirring, the mixture was diluted with water (10 mL) and extracted with Et_2O (4 × 10 mL). The water layer was then made basic by addition of a saturated aqueous $KHCO_3$ solution (pH ~ 10) and extracted with EtOAc (3× 25 mL). The combined extracts were dried over Na_2SO_4 and concentrated to afford (*Z*)-**3** (332 mg, 67%) as a light-brown solid; m.p. 92.0 – 92.9 °C; ^{1}H NMR (400 MHz, DMSO-d_6): 7.27 (d, J = 2.1 Hz, 2H; 2 arom. H), 6.96 (d, J = 8.0 Hz, 2H; 2 arom. H), 6.45 (dd, J = 8.0, 2.0 Hz, 2H; 2 arom. H), 4.84 (s, 4H; 2 NH_2), 2.78-2.64 (m, br. 8H; 4 CH_2); ^{13}C NMR (100 MHz, DMSO-d_6): 146.5, 140.5, 135.7, 134.6, 125.0, 114.2, 109.1, 34.8, 29.0; HRMS (ESI) *m/z*: 263.1543 ([M +H]$^+$, calcd for $C_{18}H_{19}N_2^+$: 263.1543).

(*E*)-1,1'-(2,2',3,3'-tetrahydro-(1,1'-biindenylidene)-6,6'-diyl)bis(3-phenylurea) [(*E*)-1]:
Phenyl isocyanate (66 μL, 0.60 mmol) was added to compound (*E*)-**3** (72 mg, 0.27 mmol) in CH_2Cl_2 (40 mL) under a N_2 atmosphere. The mixture was stirred at reflux for 3 d, after which the white precipitate was filtered off. The product was recrystallized from DMSO, washed vigorously with CH_2Cl_2 and air-dried to afford (*E*)-**1** (78 mg, 57%) as a beige solid; m.p. 260 °C (dec); ^{1}H NMR (400 MHz, DMSO-d_6): 8.71 (s, 2H; 2 NH), 8.63 (s, 2H; 2 NH), 7.89 (s, 2H; 2 arom. H), 7.46 (d, J = 8.0 Hz, 4H; 4 arom. H), 7.31-7.20 (m, 8H; 8 arom. H), 6.97 (t, J = 7.4 Hz, 2H; 2 arom. H), 3.15-3.01 (m, br. 8H; 4 CH_2); too insoluble for a ^{13}C NMR measurement; HRMS (ESI) *m/z*: 501.2275 ([M +H]$^+$, calcd for $C_{32}H_{29}N_4O_2^+$: 501.2285).

(*Z*)-1,1'-(2,2',3,3'-tetrahydro-(1,1'-biindenylidene)-6,6'-diyl)bis(3-phenylurea) [(*Z*)-1]:
Phenyl isocyanate (86 μL, 0.79 mmol) was added to compound (*Z*)-**3** (103 mg, 0.39 mmol) in CH_2Cl_2 (5 mL) under a N_2 atmosphere. The solution was stirred for 16 h, after which the white precipitate was filtered off and air-dried to afford (*Z*)-**1** (137 mg, 70%) as a white solid; m.p. 340 °C (dec); ^{1}H NMR (400 MHz, DMSO-d_6): 8.74 (s, 2H; 2 NH), 8.50 (s, 2H; 2 NH), 8.11 (d, J = 2.1 Hz, 2H; 2 arom. H), 7.46-7.40 (m, 6H; 6 arom. H), 7.23 (d, J = 8.2 Hz, 2H; 2 arom. H), 7.10 (t, J = 7.8 Hz, 4H; 4 arom. H), 6.83 (t, J = 7.4 Hz, 2H; 2 arom. H), 2.93-2.75 (m, br. 8H; 4 CH_2); ^{13}C NMR (100 MHz, DMSO-d_6): 152.6, 141.3, 140.1, 139.8, 137.5, 134.8, 128.6, 125.1, 121.5, 118.1, 117.7, 113.6, 34.4, 29.4; HRMS (ESI) *m/z*: 501.2275 ([M +H]$^+$, calcd for $C_{32}H_{29}N_4O_2^+$: 501.2285).; elemental analysis calcd (%) for $C_{32}H_{28}N_4O_2 \cdot {}^2/_5C_2H_6SO$: C 74.07, H 5.76, N 10.53; found: C 74.01, H 5.77, N 10.51.

^{1}H and ^{13}C NMR Spectra of new compounds

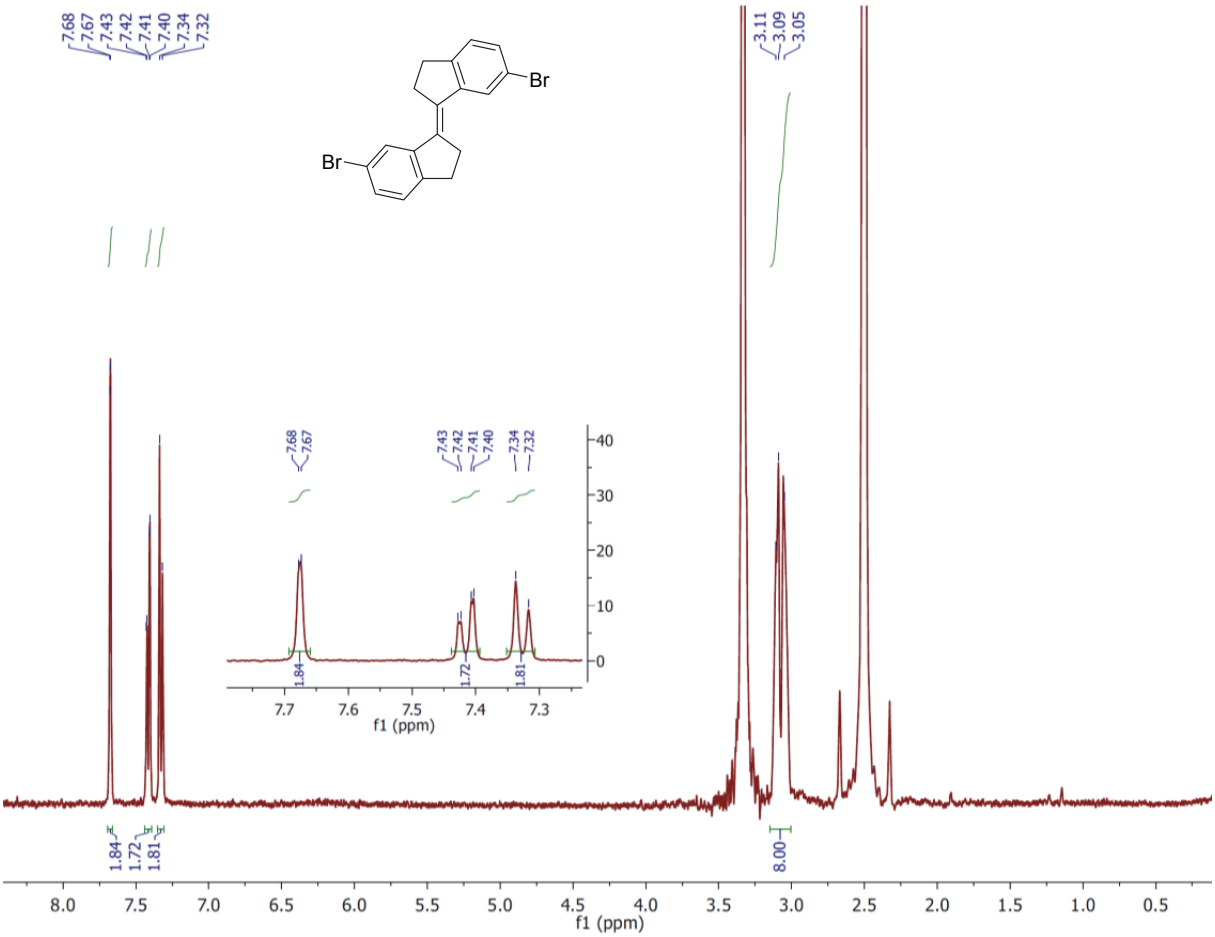

Figure S1. 400 MHz ^{1}H NMR spectrum of (*E*)-**2** measured at 298 K in DMSO-d_6.

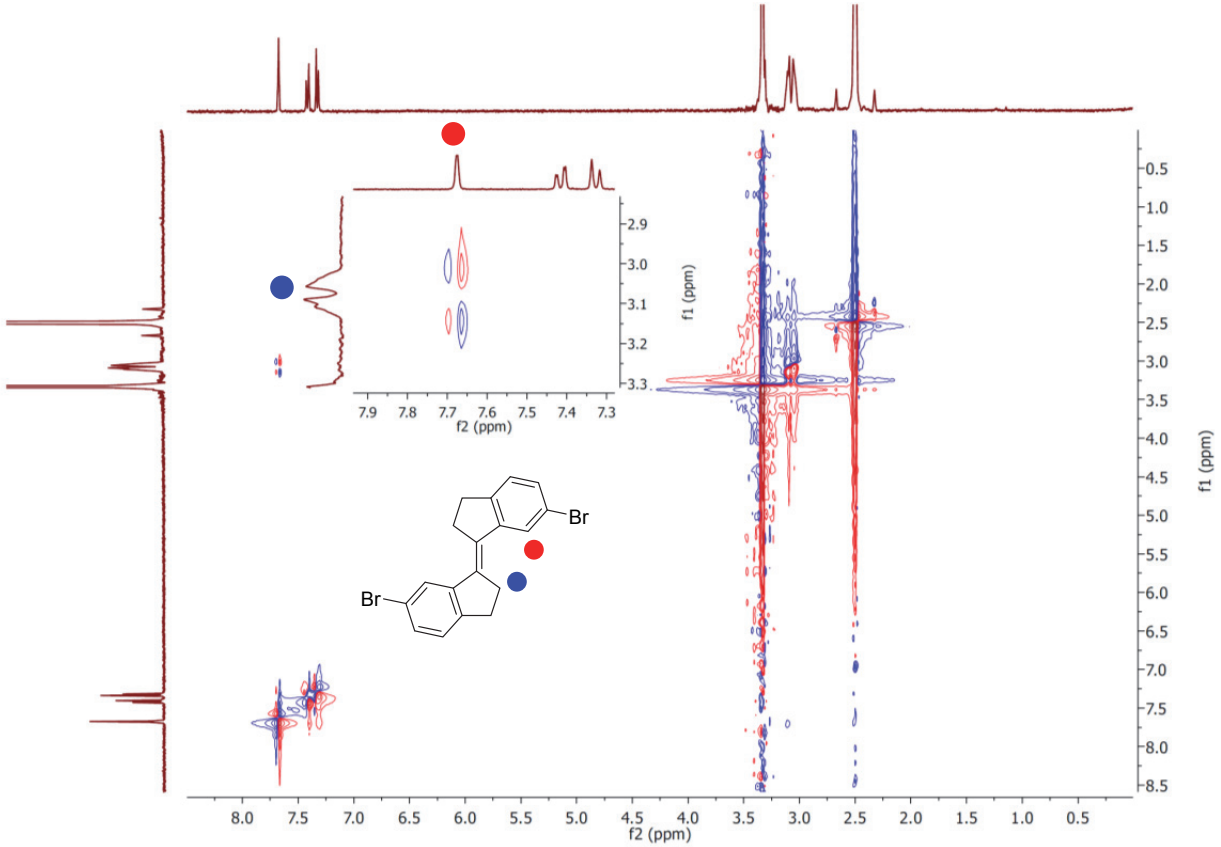

Figure S2. NOESY NMR spectrum of (*E*)-**2** measured at 298 K in DMSO-d_6.

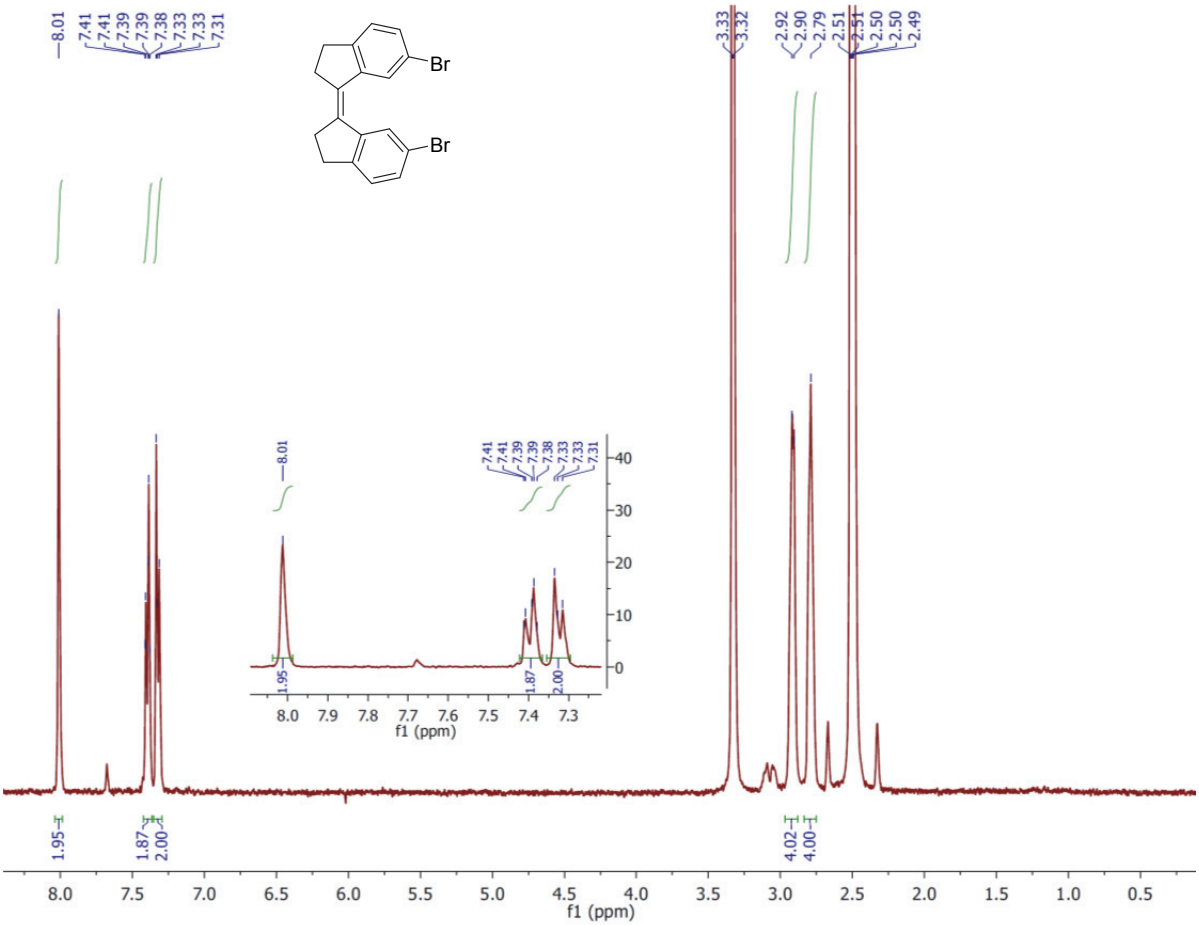

Figure S3. 400 MHz ^{1}H NMR spectrum of (*Z*)-**2** measured at 298 K in DMSO-d_6.

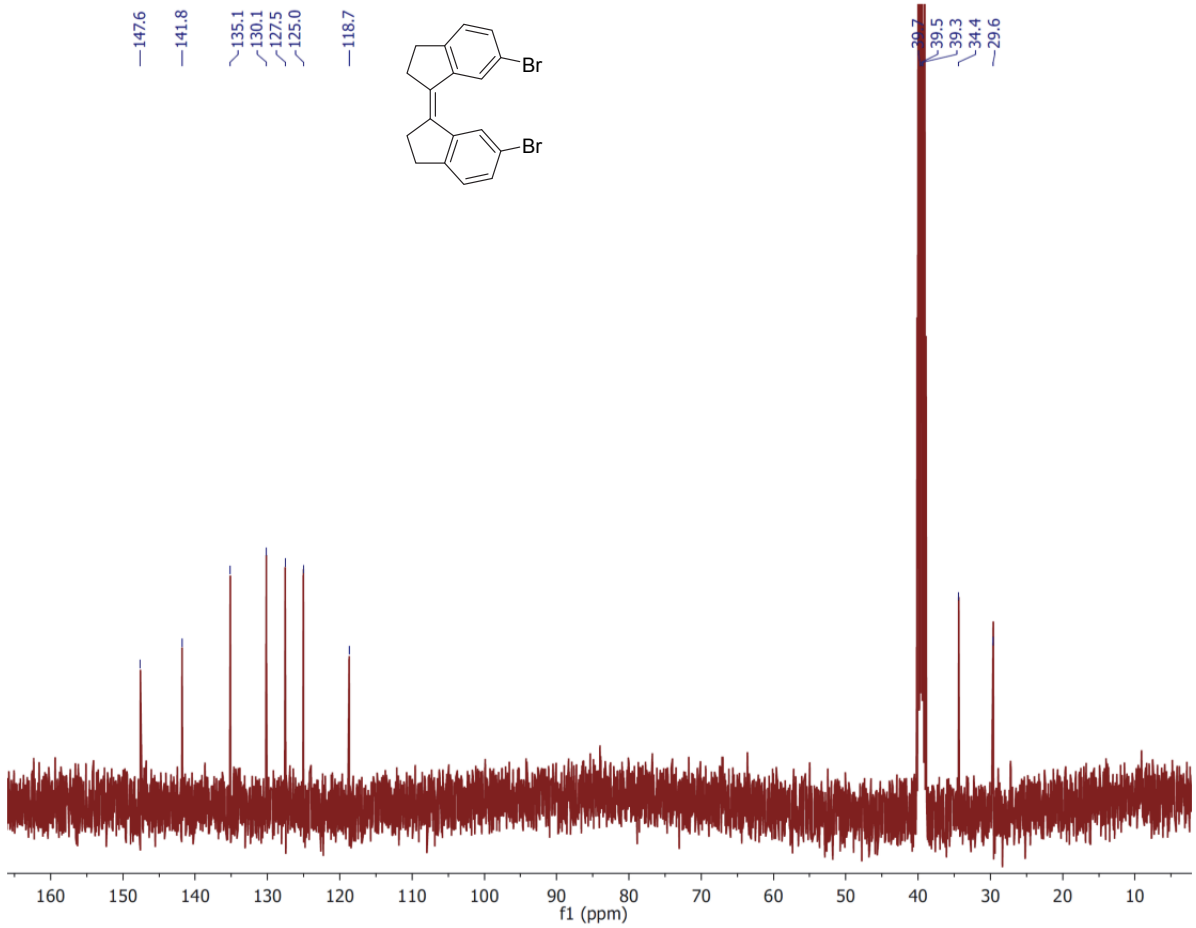

Figure S4. 100 MHz ^{13}C NMR spectrum of (*Z*)-**2** measured at 298 K in DMSO-d_6.

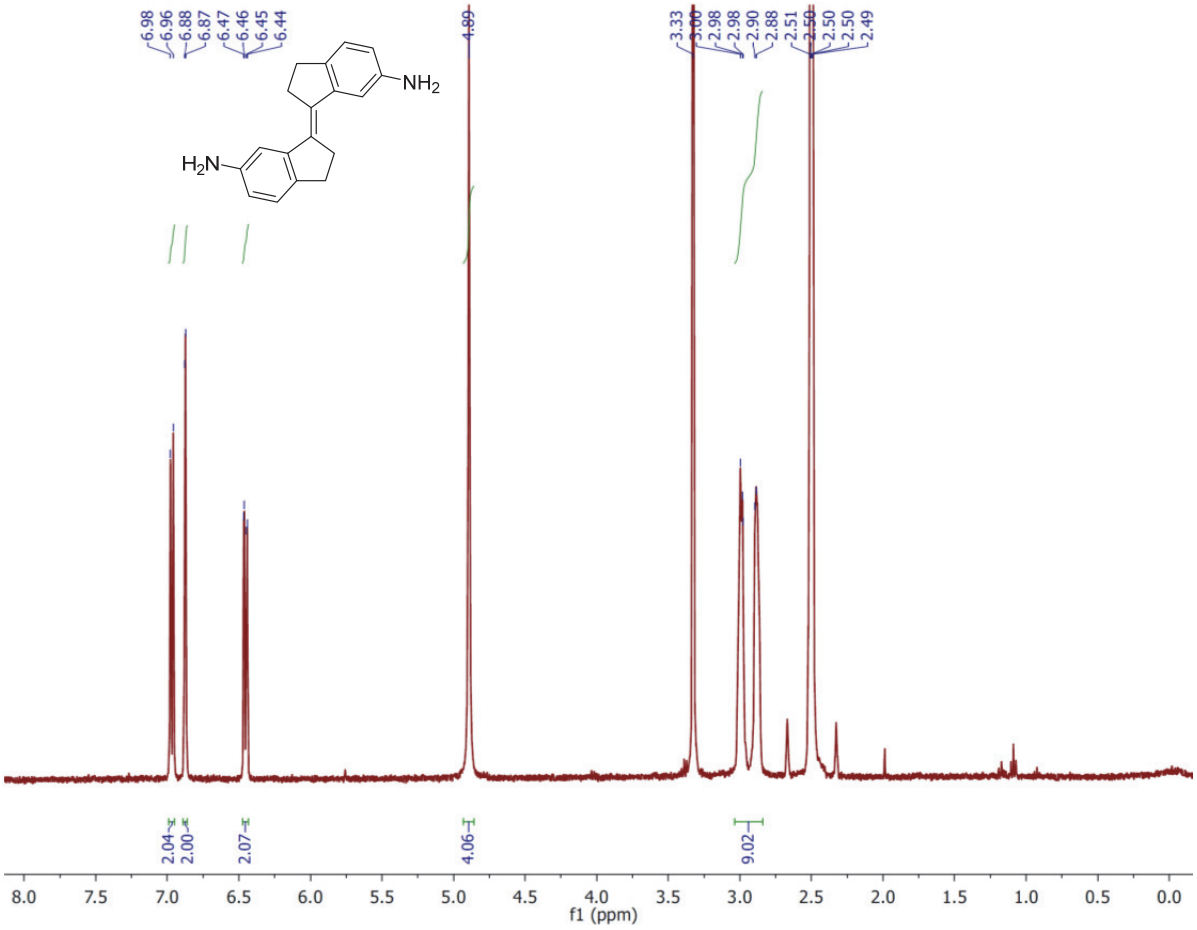

Figure S5. 400 MHz ^{1}H NMR spectrum of (*E*)-**3** measured at 298 K in DMSO-d_6.

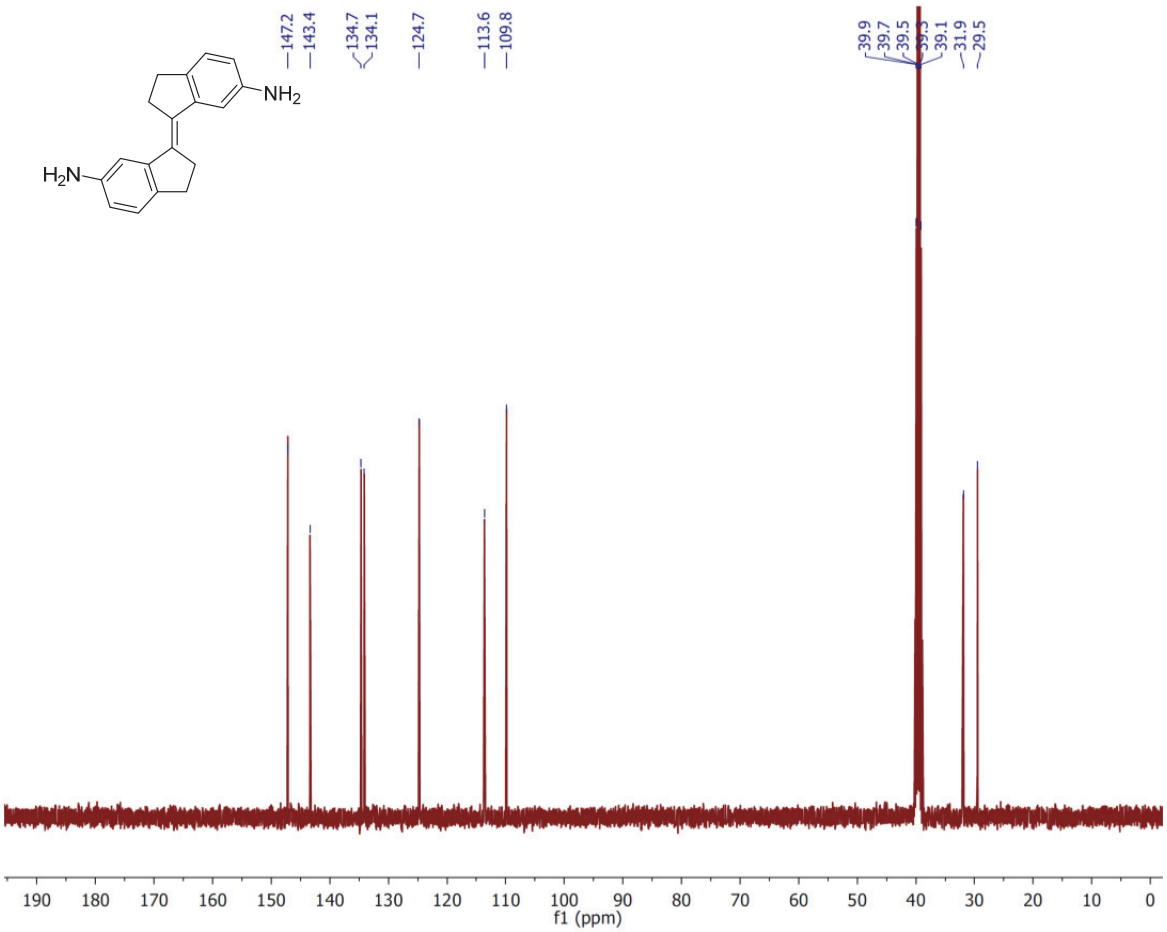

Figure S6. 100 MHz ^{13}C NMR spectrum of (*E*)-**3** measured at 298 K in DMSO-d_6.

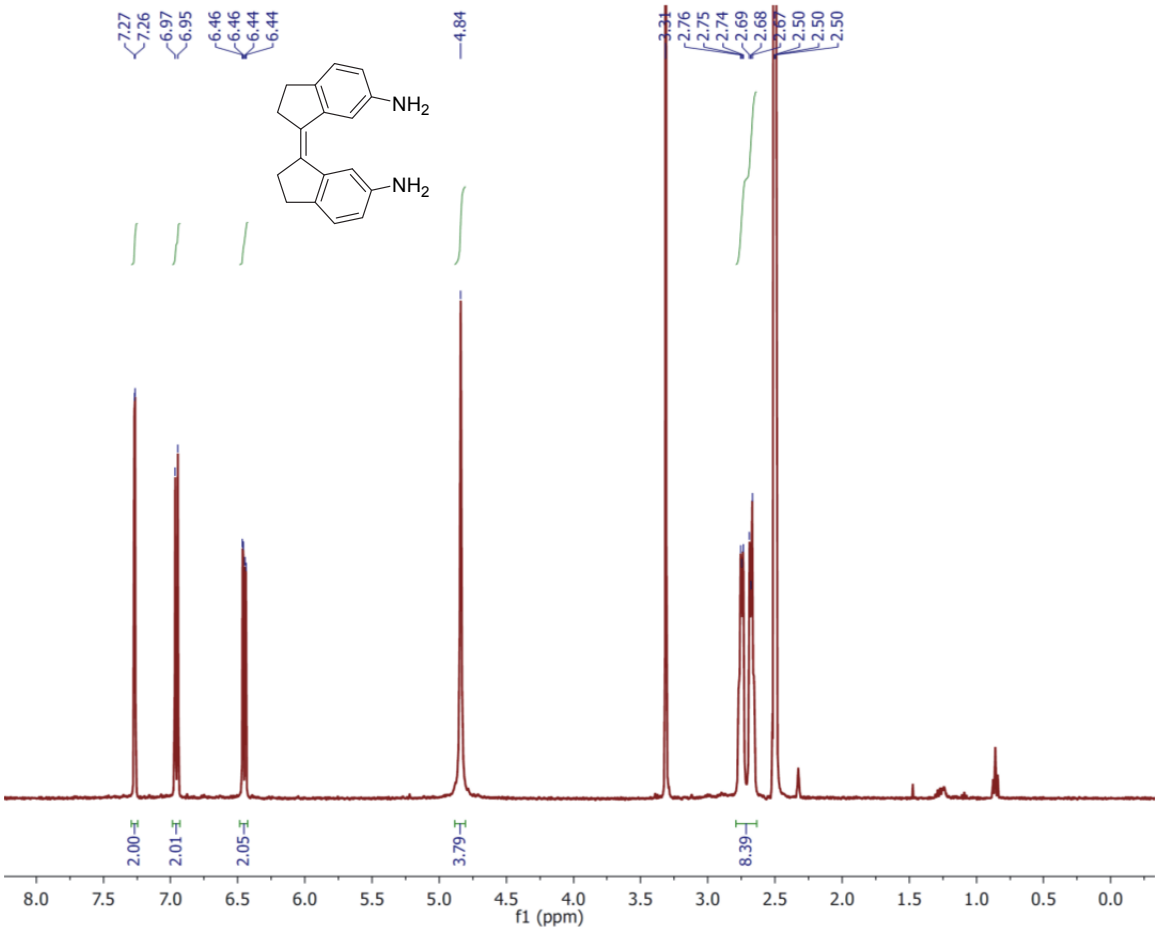

Figure S7. 400 MHz ^{1}H NMR spectrum of (*Z*)-**3** measured at 298 K in DMSO-d_6.

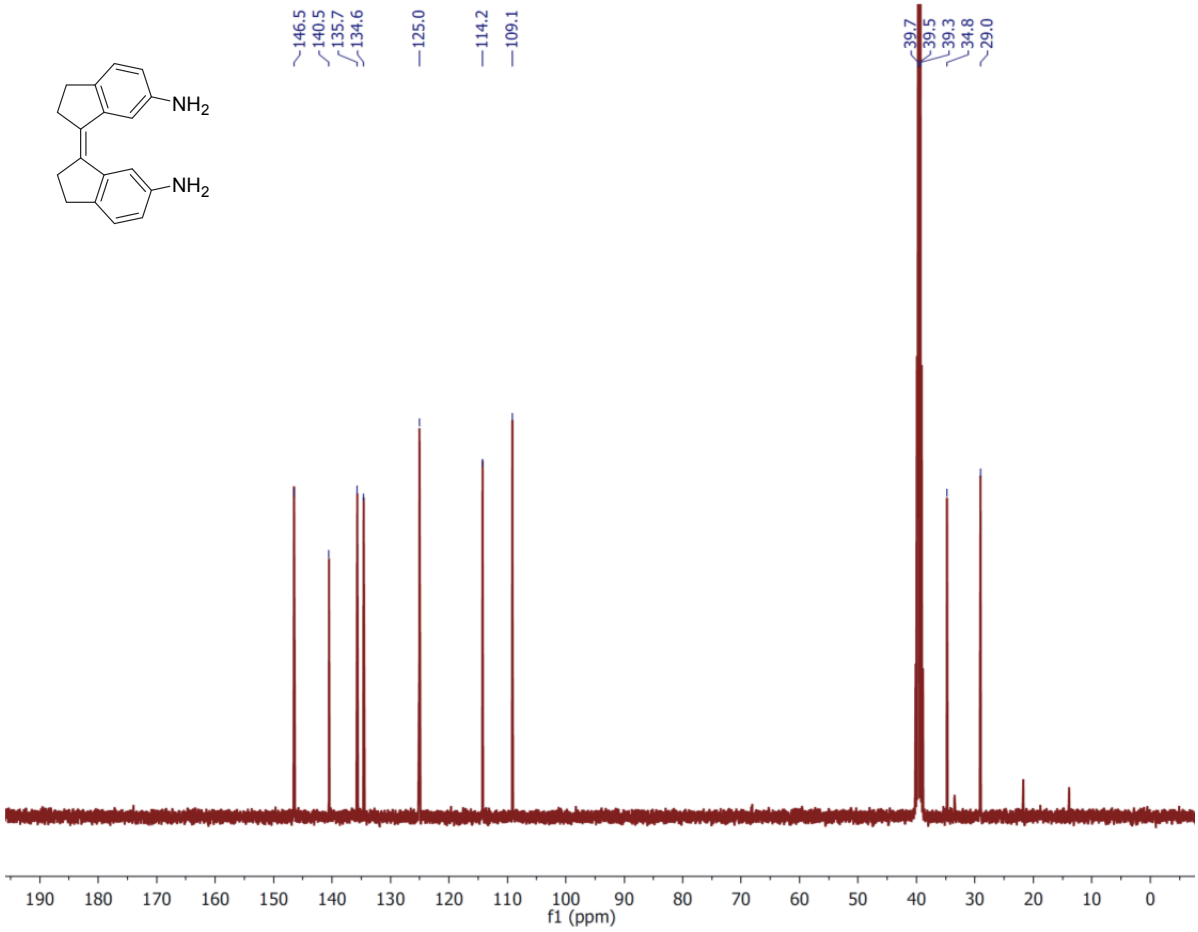

Figure S8. 100 MHz ^{13}C NMR spectrum of (*Z*)-**3** measured at 298 K in DMSO-d_6.

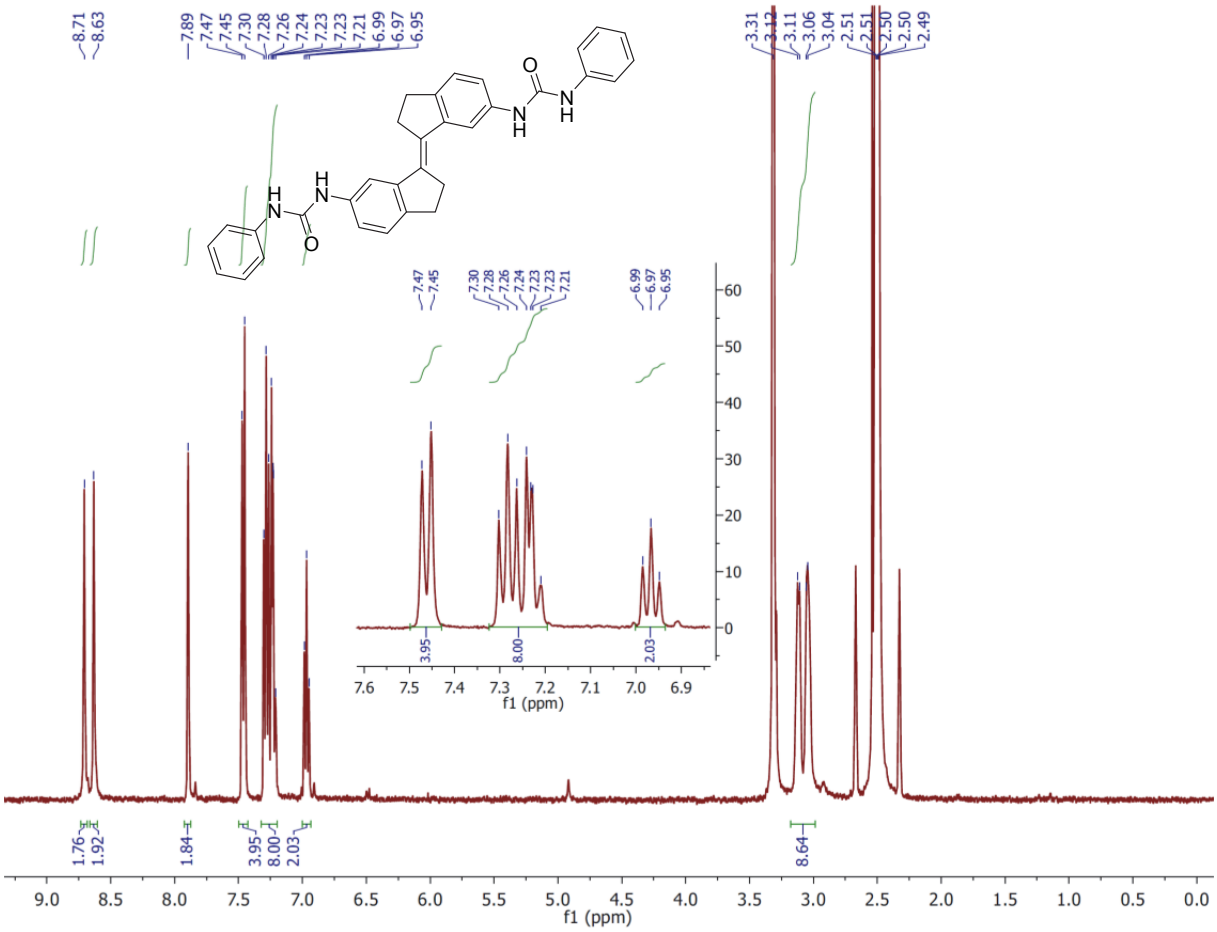

Figure S9. 400 MHz ^{1}H NMR spectrum of (*E*)-**1** measured at 298 K in DMSO-d_6.

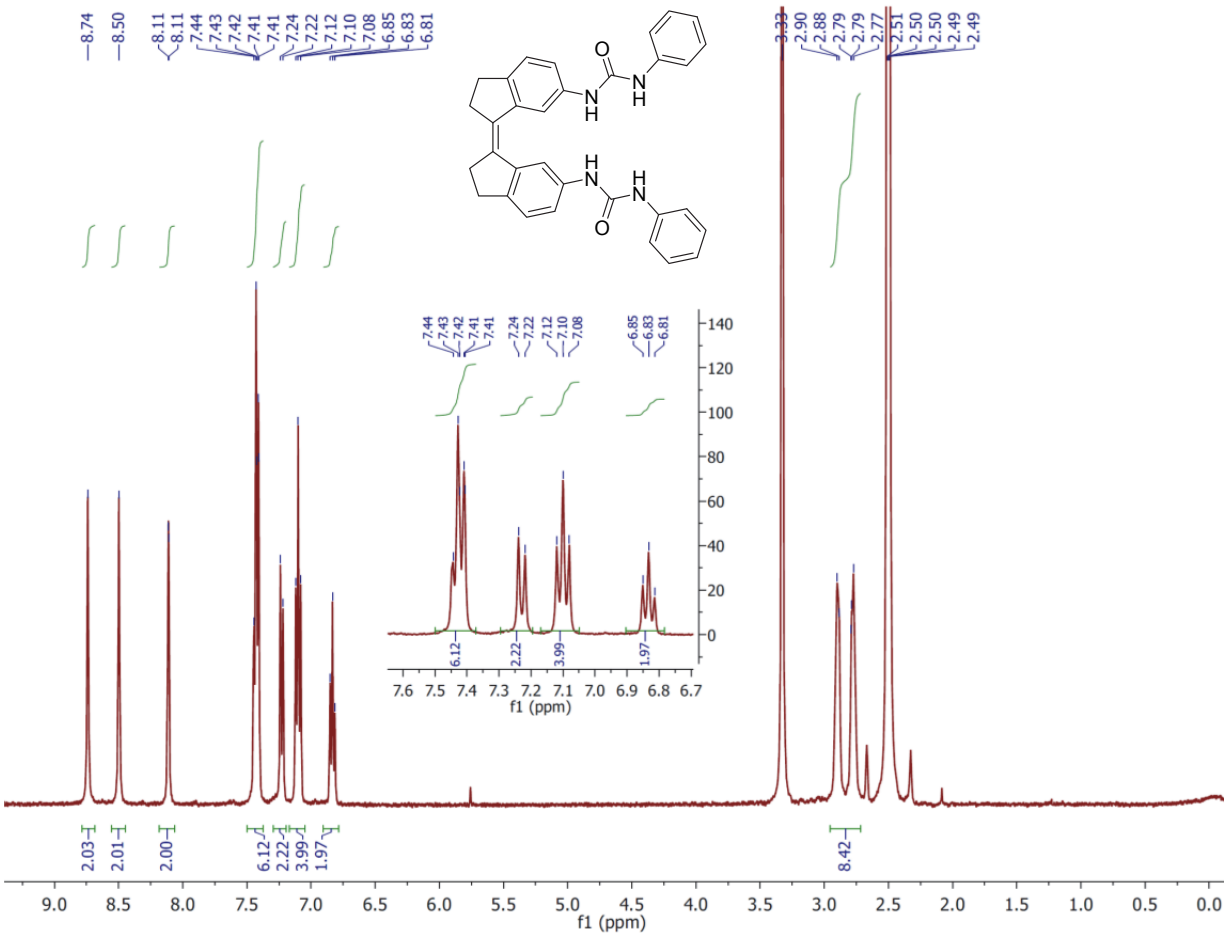

Figure S10. 400 MHz ^{1}H NMR spectrum of (*Z*)-**1** measured at 298 K in DMSO-d_6.

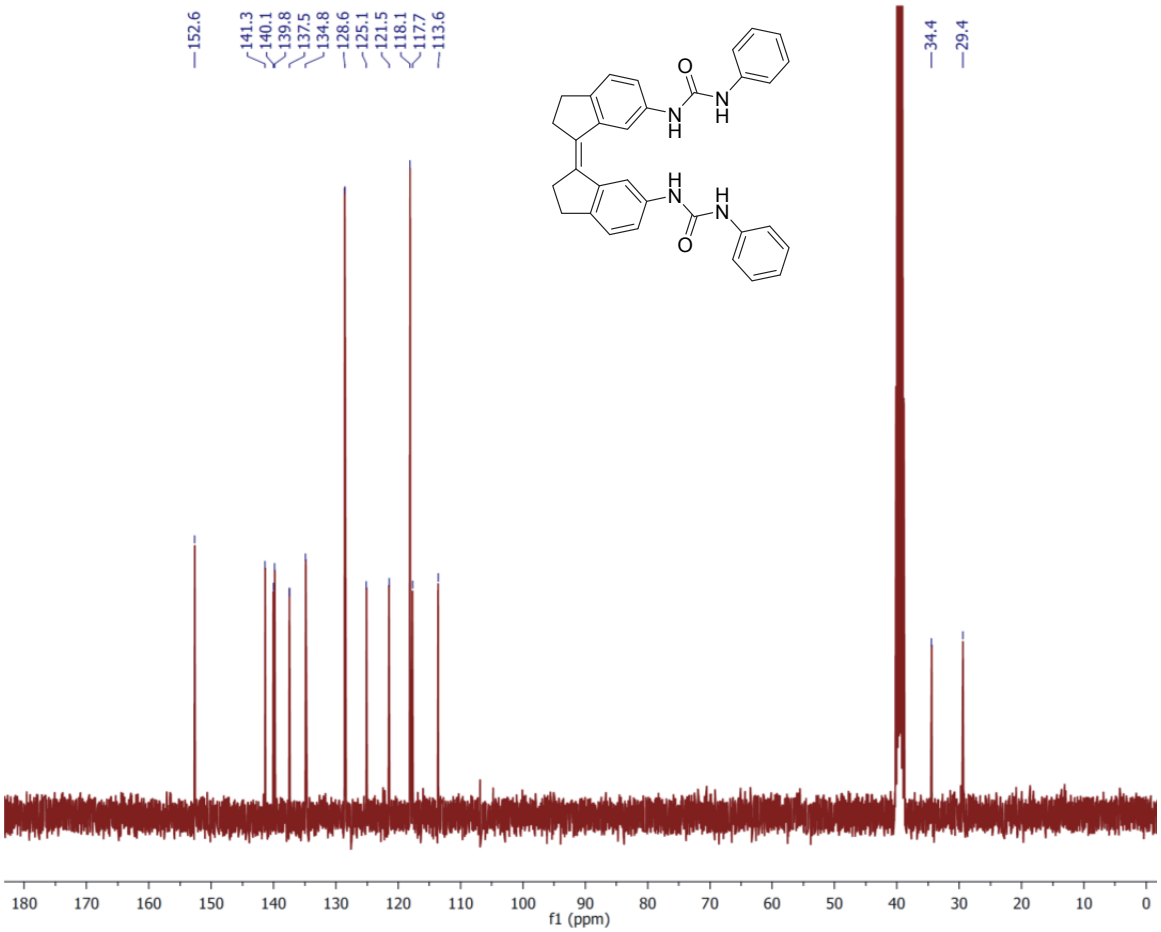

Figure S11. 100 MHz ^{13}C NMR spectrum of (*Z*)-**1** measured at 298 K in DMSO-d_6.

^{1}H NMR photoisomerization studies

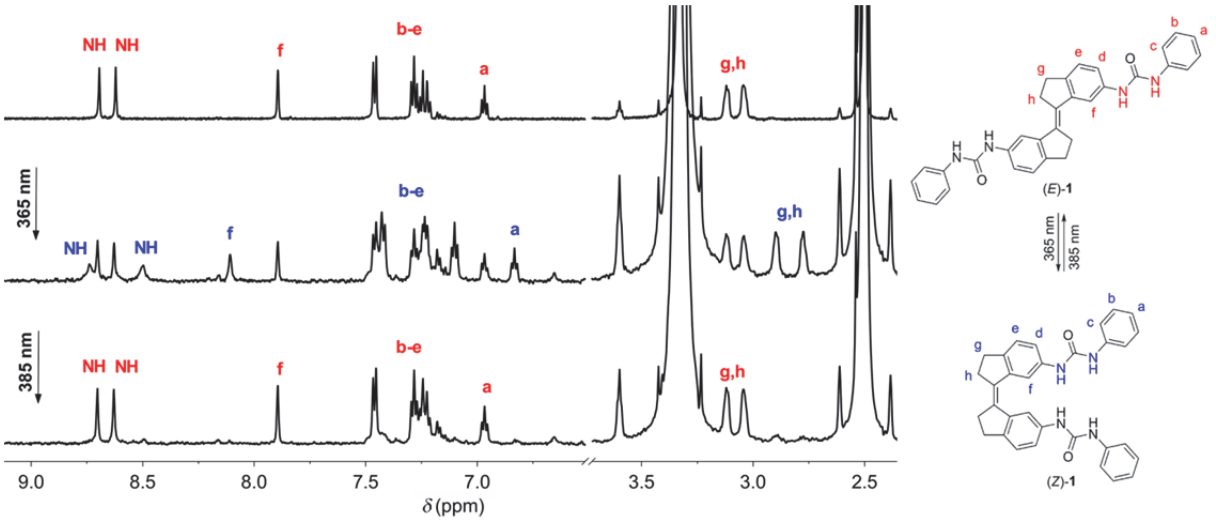

Figure S12. Aromatic and aliphatic region in the ^{1}H NMR spectrum (600 MHz, 293 K) of (*E*)-**1** in degassed DMSO-d_6 (2.5×10^{-4} M) (top) and spectral changes after irradiation with 365 nm light for 1 h (middle) followed by irradiation with 385 nm light for 1 h (bottom) at 20 °C. For determination of the PSS ratios, the integrals of the NH, H_a and H_f signals were averaged giving a PSS_{365} ratio (*E*/*Z*) of 49:51 and a PSS_{385} ratio (*E*/*Z*) of 93:7.

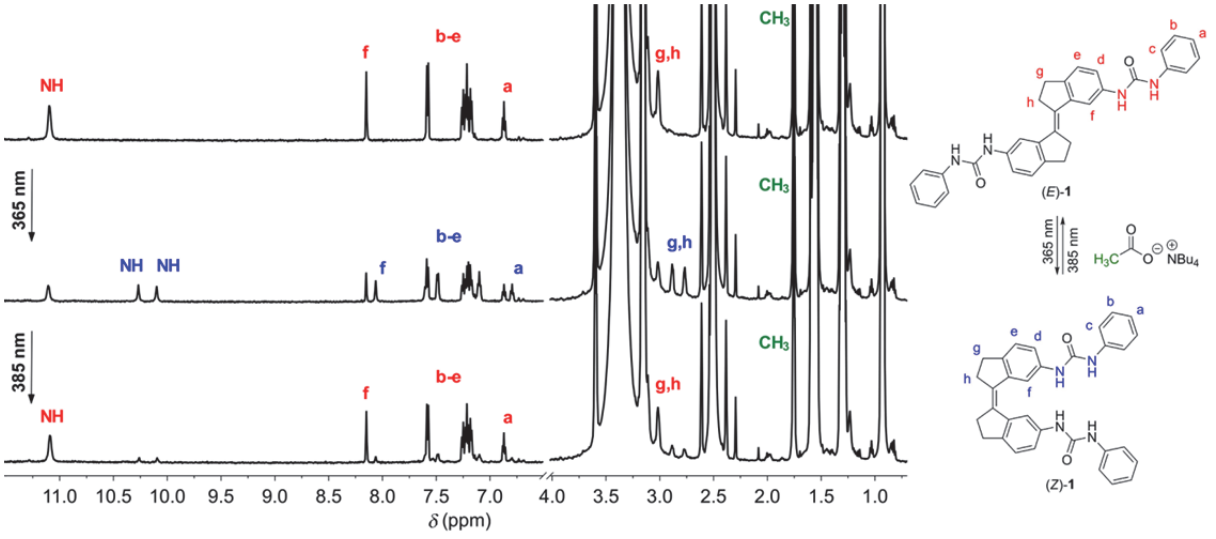

Figure S13. Aromatic and aliphatic region in the ^{1}H NMR spectrum (600 MHz, 293 K) of a mixture of (*E*)-**1** (2.5×10^{-4} M) and $[Bu_4N]^+[CH_3CO_2]^-$ (2.5×10^{-3} M) in degassed DMSO-d_6/0.5% H_2O (top) and spectral changes after irradiation with 365 nm light for 1 h (middle) followed by irradiation with 385 nm light for 1 h (bottom) at 20 °C. For determination of the PSS ratios, the integrals of the NH, H_a and H_f signals were averaged giving a PSS_{365} ratio (*E*/*Z*) of 48:52 and a PSS_{385} ratio (*E*/*Z*) of 88:12.

Quantum yield determination

The photon flux of the Thorlab model F365F1 high-power LED (λ_{max} = 365 nm) was estimated by measuring the production of ferrous ions from potassium ferrioxalate.[2] The rate (r) of Fe^{2+} ion formation was: 8.81×10^{-7} M s^{-1}. Hence, the moles of photons absorbed per time unit ($Nh\nu/t$ = moles of $Fe^{2+}/\phi\, t$) in a 2 mL solution can be calculated using the reported quantum yield of ferrioxalate ($\phi = 1.21$),[3] which gives: 1.46×10^{-9} mol s^{-1}.

A solution of (*E*)-**1** in DMSO (1×10^{-4} M) in a 1 cm quartz cuvette was irradiated at 20 °C with the Thorlab model F365F1 high-power LED. The concentration was high enough to absorb all incident light ($Abs_{365} \geq 2$). The absorbance increase at λ = 380 nm was monitored over time by UV-vis spectroscopy and the molar absorptivities at this wavelength (ε_E = 2468.4 M^{-1} cm^{-1}, ε_Z = 7365.5 M^{-1} cm^{-1}) were used to calculate the concentration of (*Z*)-**1**. The slopes of the plots of the concentration increase versus time (Figure S12), at low conversion, represent the rate of formation (r). These were obtained by linear fitting to the equation y = ax +b using Origin software. The photochemical quantum yield was obtained by comparison of the rate of formation of (*Z*)-**1** ($r = 3.64 \times 10^{-8}$ M s^{-1}) with the rate of Fe^{2+} formation from potassium ferrioxalate giving $\phi_{Z\rightarrow E}$ = 5.0 ± 0.15%. The quantum yield for the 'backward' reaction is defined as: $\phi_{Z\rightarrow E} = \phi_{E\rightarrow Z}\, \varepsilon_E\, n_E / \varepsilon_Z\, n_Z$, where ε_E,ε_Z are the molar absorptivities at λ = 365 nm (ε_E = 27945 M^{-1} cm^{-1}, ε_Z = 16834 M^{-1} cm^{-1}) and n_E,n_Z are the amount of (*E*)-**1** and (*Z*)-**1** at the photostationary state (PSS_{365} *E*/*Z* = 49:51), giving $\phi_{Z\rightarrow E}$ = 8.0 ± 0.23%.

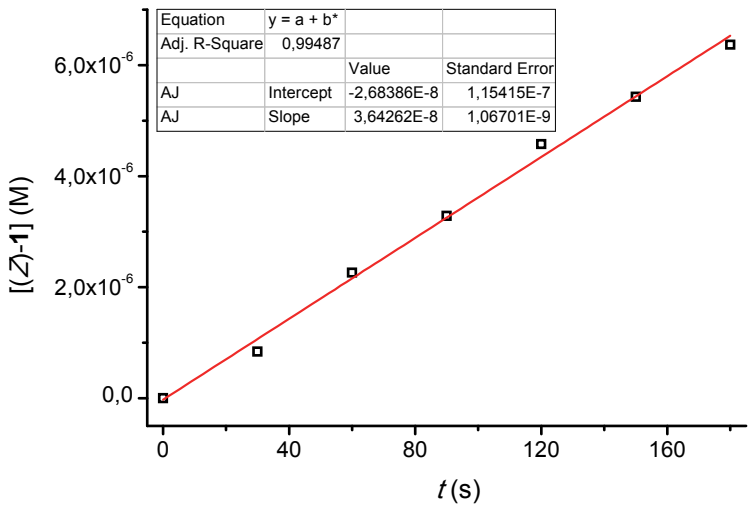

Figure S14. Concentration of (*Z*)-**1** as a function of time during λ = 365 nm irradiation of a 1×10^{-4} M solution (2 mL) obtained by measuring the absorbance increase at λ = 380 nm.

^{1}H NMR titration experiments

First, 5 mM solutions of receptors (*E*)-**1** and (*Z*)-**1** were prepared in DMSO-d_6/0.5%H_2O (v/v). The tetrabutylammonium anion was dissolved in the receptor solution and was present at a 50 mM concentration. The 50 mM anion solution was added stepwise to 0.5 mL of the 5 mM receptor solution and a ^{1}H NMR spectrum (400 MHz) was recorded after each addition.

Addition of $[Bu_4N]^+[Cl]^-$ to (*Z*)-1:

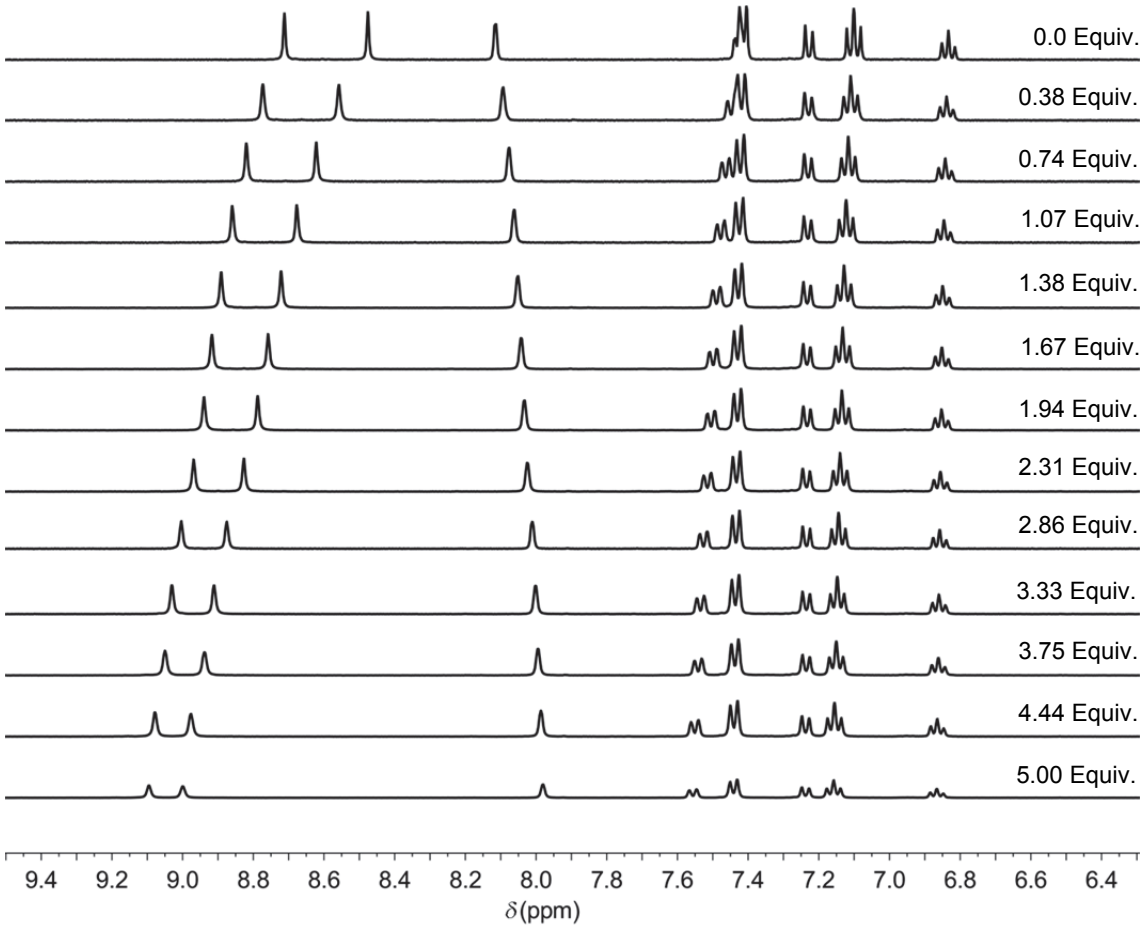

Figure S15. ^{1}H NMR spectral changes (400 MHz, 293 K) in the aromatic region of (*Z*)-**1** (5×10^{-3} M in DMSO-d_6/0.5%H_2O) upon the stepwise addition of $[Bu_4N]^+[Cl]^-$ (from top to bottom: 0.0, 0.38, 0.74, 1.07, 1.38, 1.67, 1.94, 2.31, 2.86, 3.33, 3.75, 4.44, 5.00 equivalents).

Addition of $[Bu_4N]^+[Br]^-$ to (*Z*)-1:

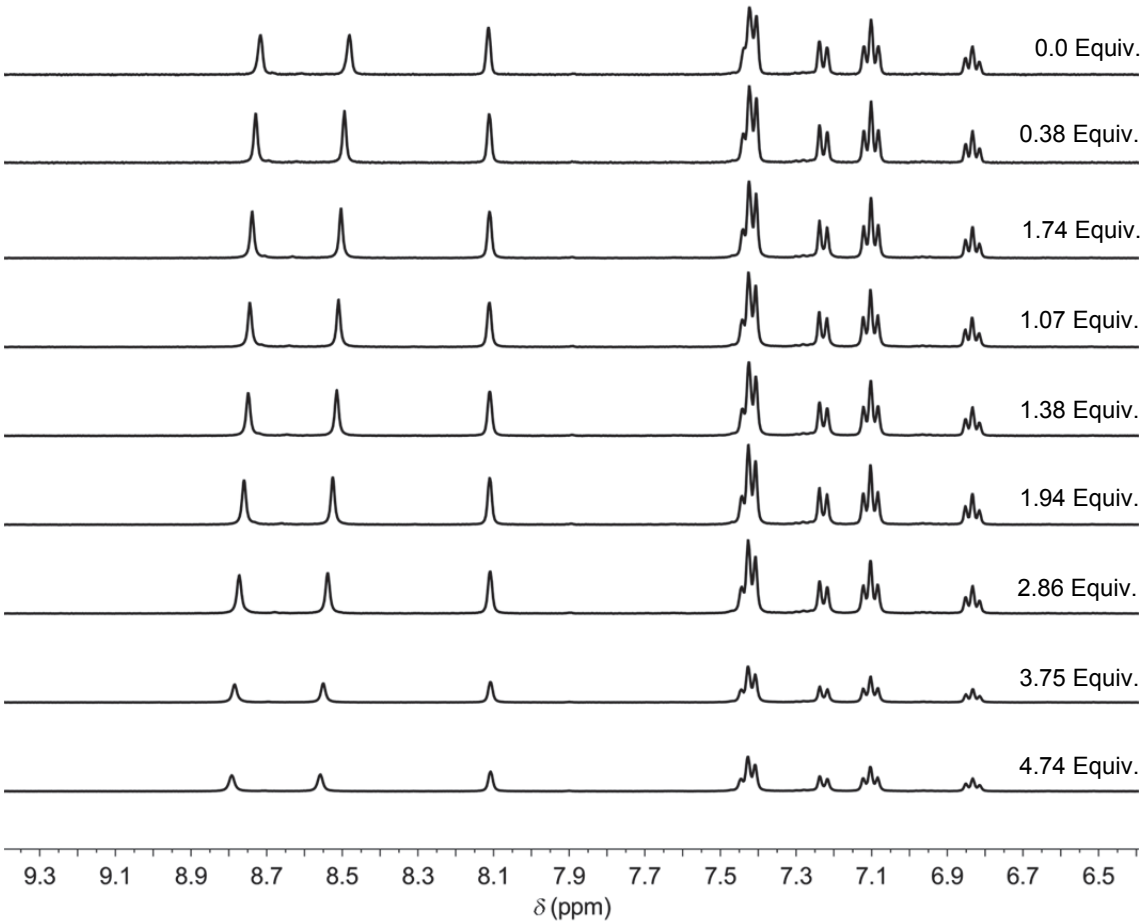

Figure S16. ^{1}H NMR spectral changes (400 MHz, 293 K) in the aromatic region of (*Z*)-**1** (5×10^{-3} M in DMSO-d_6/0.5%H_2O) upon the stepwise addition of $[Bu_4N]^+[Br]^-$ (from top to bottom: 0.0, 0.38, 0.74, 1.07, 1.38, 1.94, 2.86, 3.75, 4.74 equivalents).

Addition of $[Bu_4N]^+[NO_3]^-$ to (*Z*)-1:

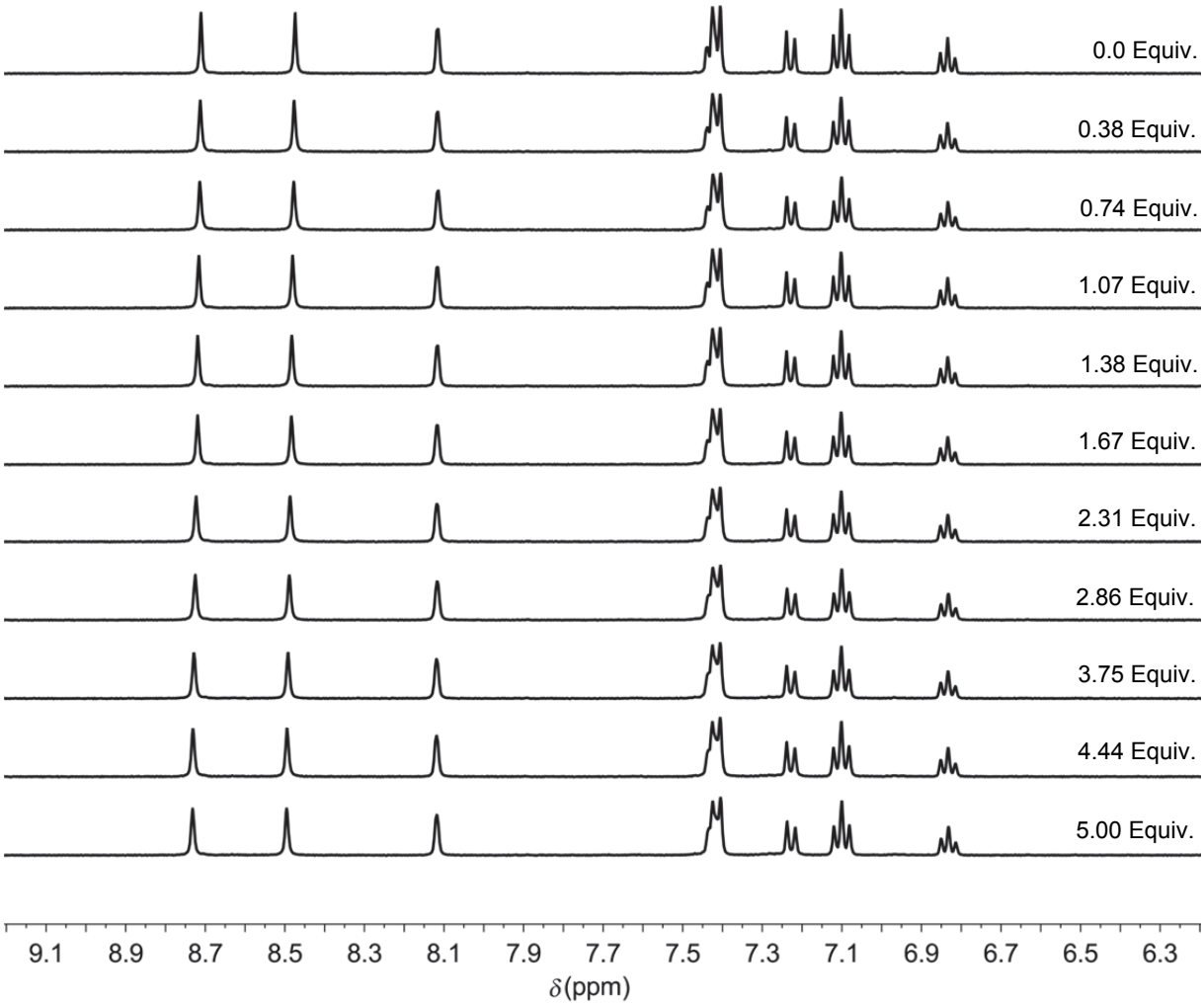

Figure S17. ^{1}H NMR spectral changes (400 MHz, 293 K) in the aromatic region of (*Z*)-**1** (5×10^{-3} M in DMSO-d_6/0.5%H_2O) upon the stepwise addition of $[Bu_4N]^+[NO_3]^-$ (from top to bottom: 0.0, 0.38, 0.74, 1.07, 1.38, 1.67, 2.31, 2.86, 3.75, 4.44, 5.00 equivalents).

Addition of $[Bu_4N]^+[CH_3CO_2]^-$ to (*Z*)-1:

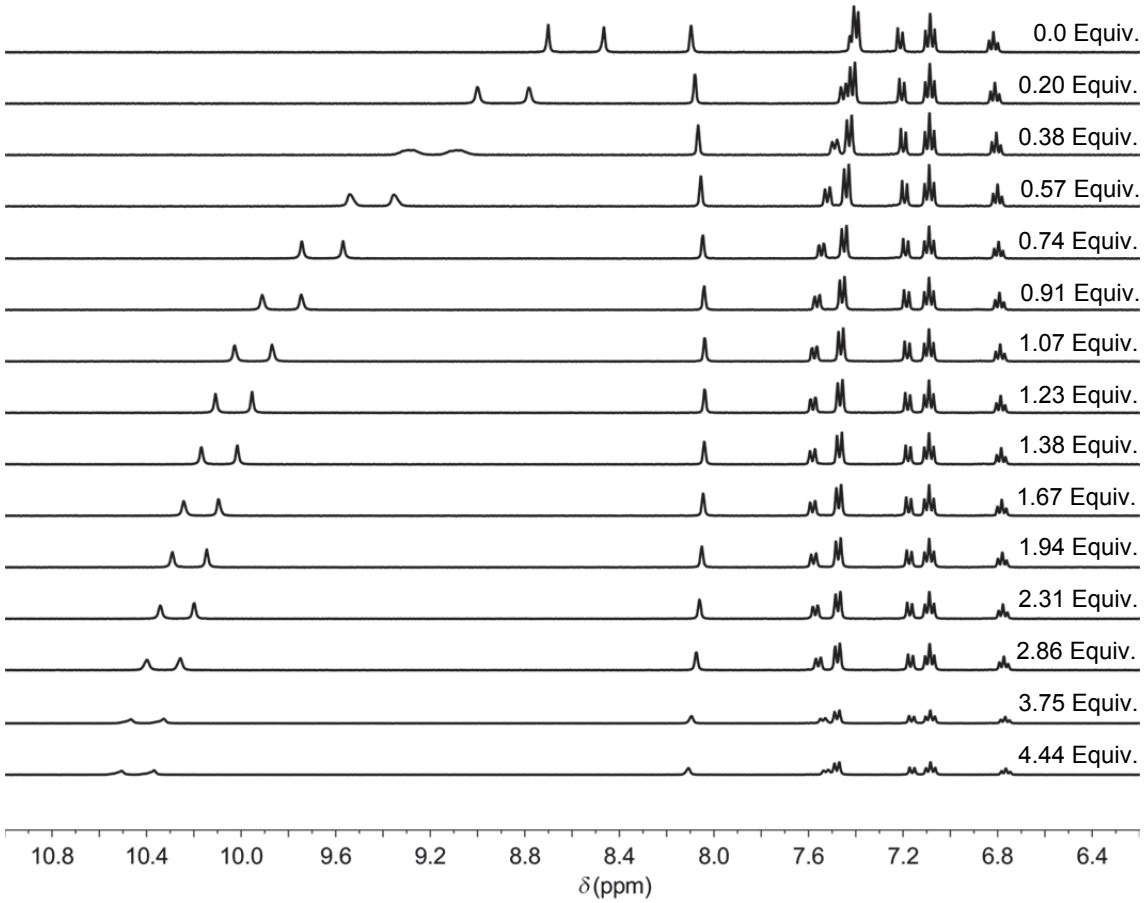

Figure S18. ^{1}H NMR spectral changes (400 MHz, 293 K) in the aromatic region of (*Z*)-**1** (5×10^{-3} M in DMSO-d_6/0.5%H_2O) upon the stepwise addition of $[Bu_4N]^+[CH_3CO_2]^-$ (from top to bottom: 0.0, 0.20, 0.38, 0.57, 0.74, 0.91, 1.07, 1.23, 1.38, 1.67, 1.94, 2.31, 2.86, 3.75, 4.44 equivalents).

Addition of $[Bu_4N]^+[H_2PO_4]^-$ to (*Z*)-1:

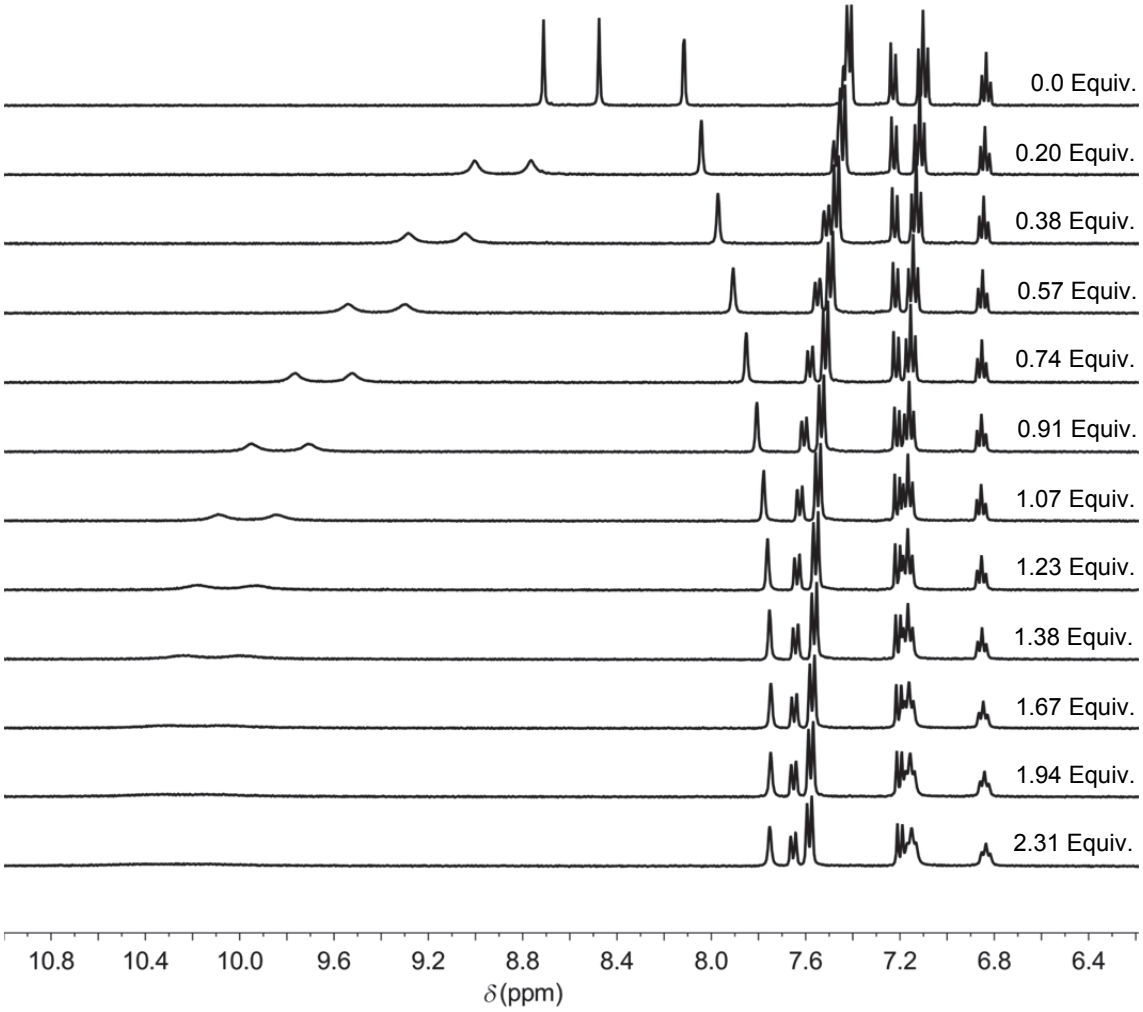

Figure S19. ^{1}H NMR spectral changes (400 MHz, 293 K) in the aromatic region of (*Z*)-**1** (5×10^{-3} M in DMSO-d_6/0.5%H_2O) upon the stepwise addition of $[Bu_4N]^+[H_2PO_4]^-$ (from top to bottom: 0.0, 0.20, 0.38, 0.57, 0.74, 0.91, 1.07, 1.23, 1.38, 1.67, 1.94, 2.31 equivalents).

Addition of $[Bu_4N]^+[HSO_4]^-$ to (*Z*)-1:

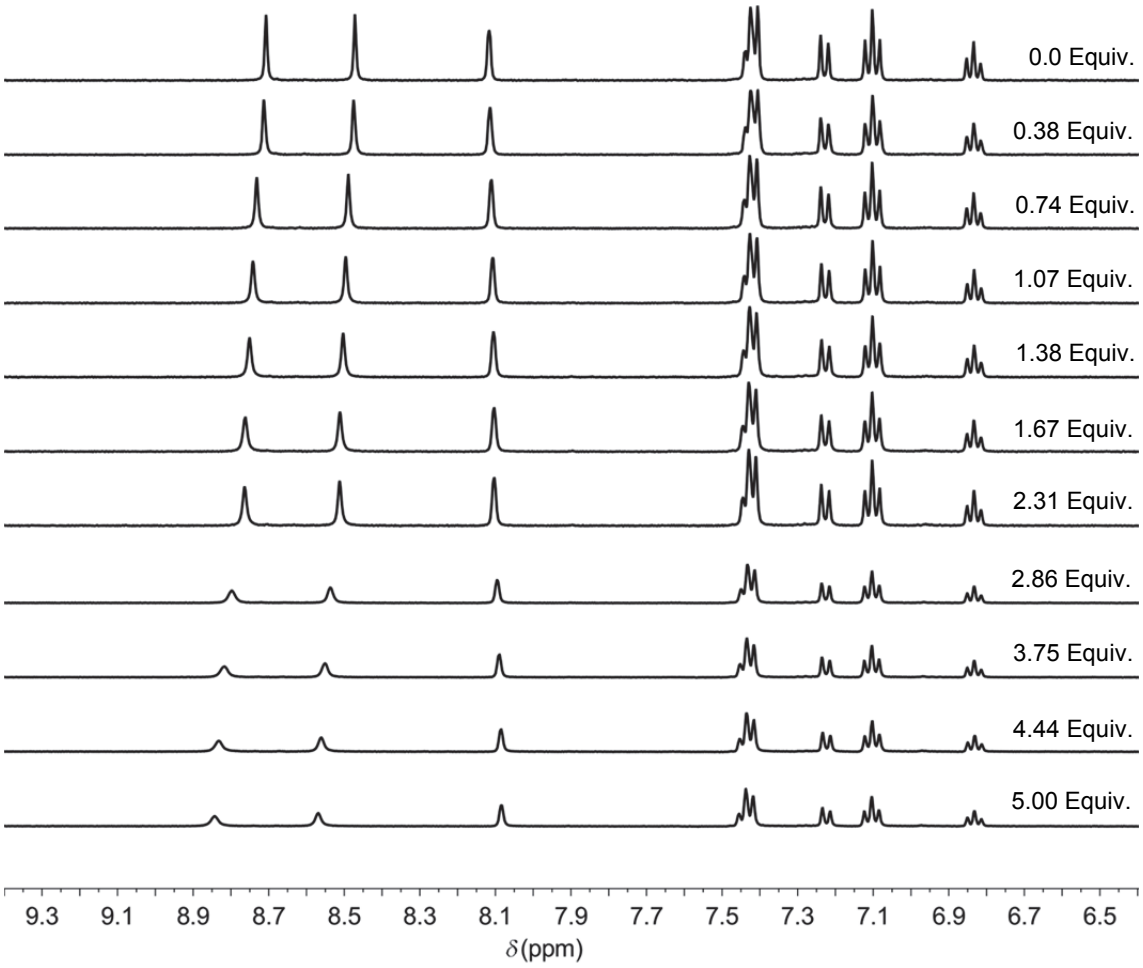

Figure S20. ^{1}H NMR spectral changes (400 MHz, 293 K) in the aromatic region of (*Z*)-**1** (5×10^{-3} M in DMSO-d_6/0.5%H_2O) upon the stepwise addition of $[Bu_4N]^+[HSO_4]^-$ (from top to bottom: 0.0, 0.38, 0.74, 1.07, 1.38, 1.67, 2.31, 2.68, 3.75, 4.44, 5.00 equivalents).

Addition of $[Bu_4N]^+[Cl]^-$ to (*E*)-1:

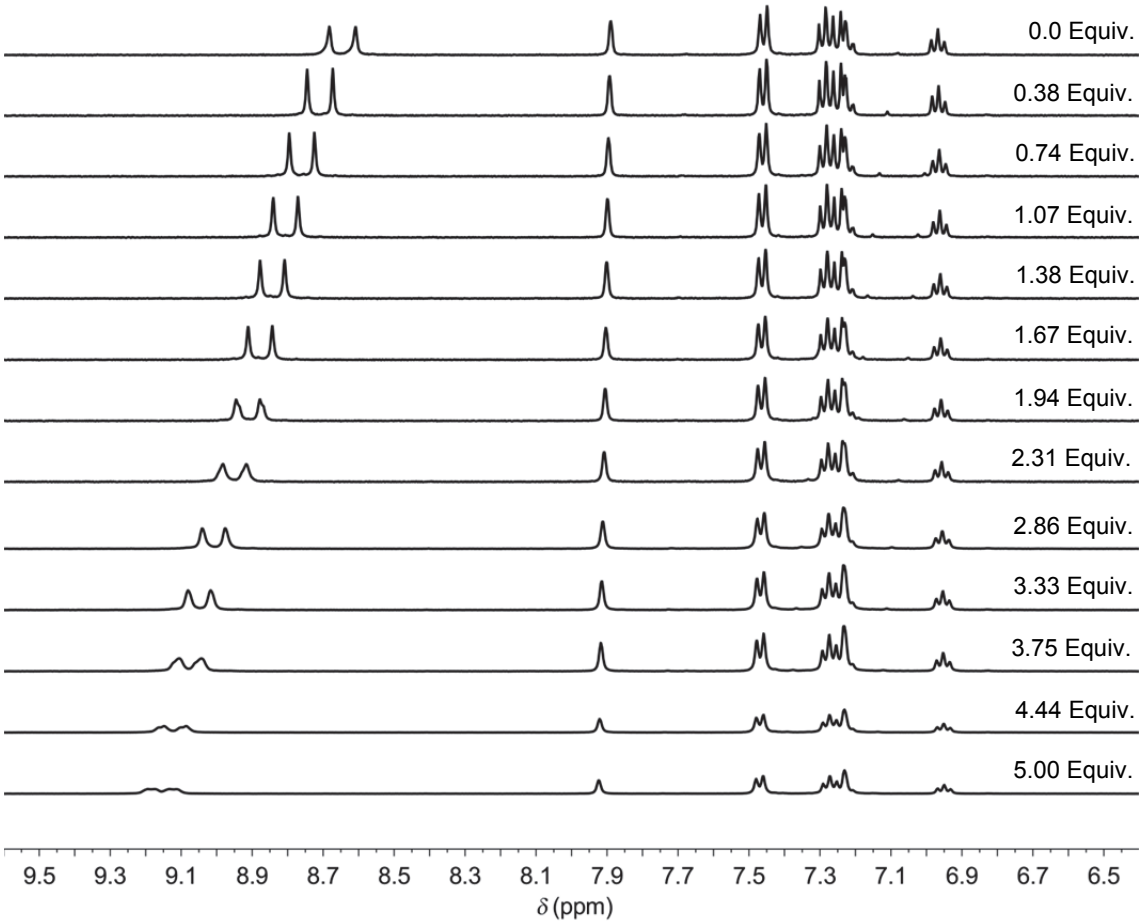

Figure S21. ^{1}H NMR spectral changes (400 MHz, 293 K) in the aromatic region of (*E*)-**1** (5×10^{-3} M in DMSO-d_6/0.5%H_2O) upon the stepwise addition of $[Bu_4N]^+[Cl]^-$ (from top to bottom: 0.0, 0.38, 0.74, 1.07, 1.38, 1.67, 1.94, 2.31, 2.86, 3.33, 3.75, 4.44, 5.00 equivalents).

Addition of $[Bu_4N]^+[CH_3CO_2]^-$ to (*E*)-1:

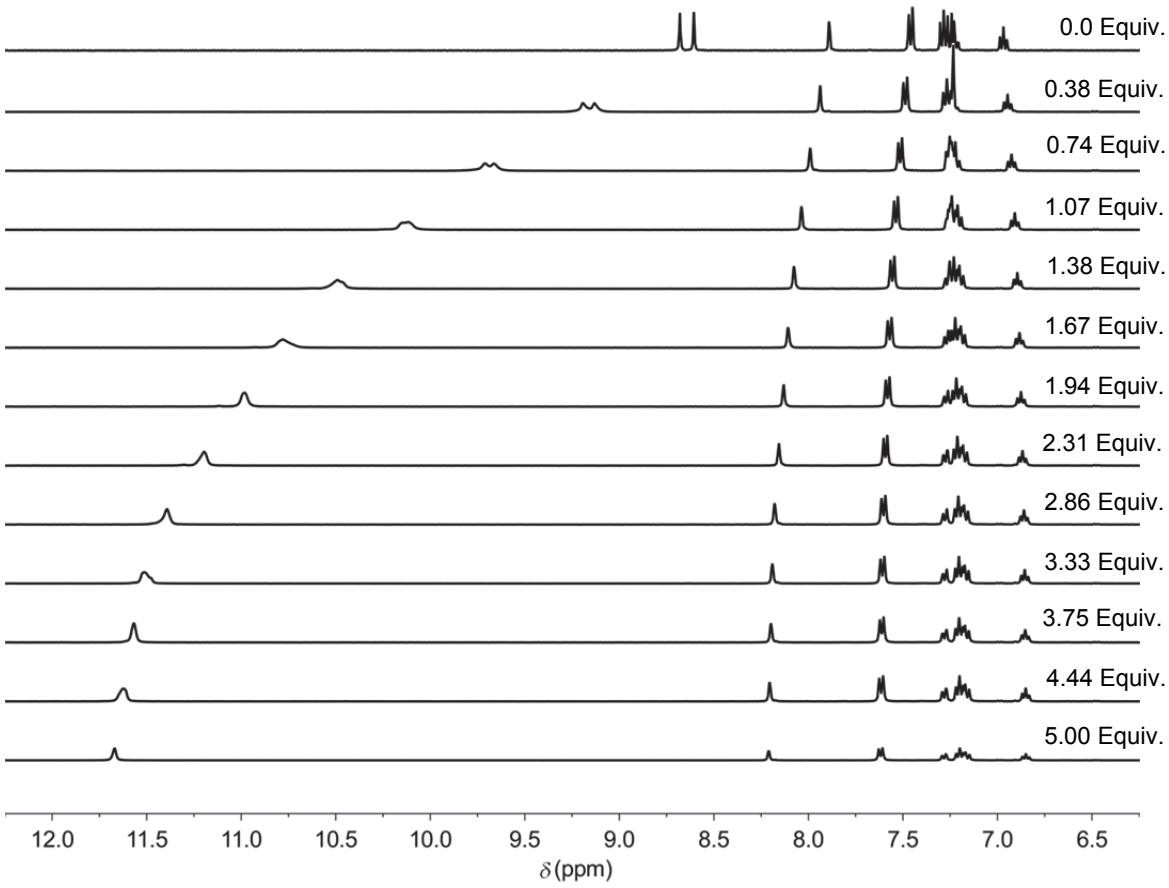

Figure S22. ^{1}H NMR spectral changes (400 MHz, 293 K) in the aromatic region of (*E*)-**1** (5×10^{-3} M in DMSO-d_6/0.5%H_2O) upon the stepwise addition of $[Bu_4N]^+[CH_3CO_2]^-$ (from top to bottom: 0.0, 0.38, 0.74, 1.07, 1.38, 1.67, 1.94, 2.31, 2.86, 3.33, 3.75, 4.44, 5.00 equivalents).

Addition of $[Bu_4N]^+[H_2PO_4]^-$ to (*E*)-1:

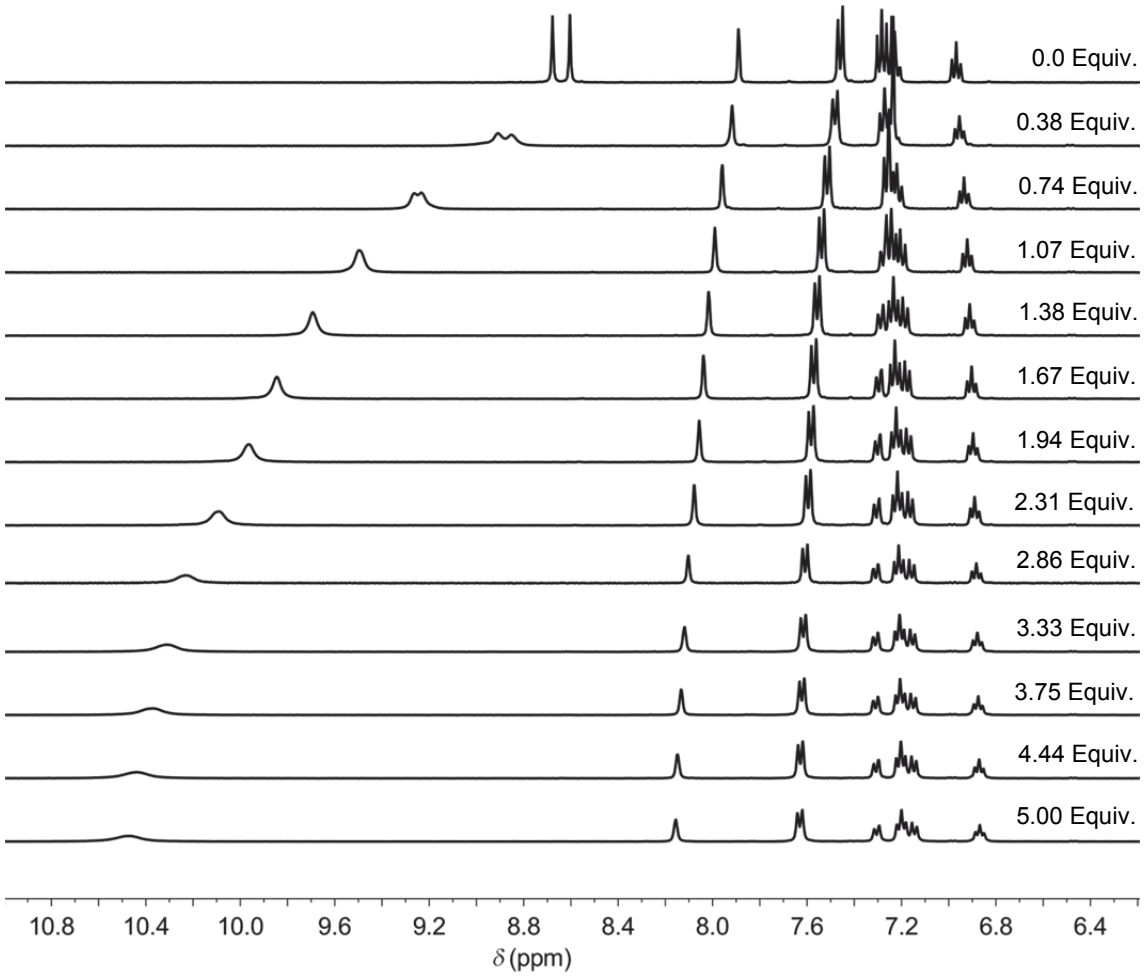

Figure S23. ^{1}H NMR spectral changes (400 MHz, 293 K) in the aromatic region of (*E*)-**1** (5×10^{-3} M in DMSO-d_6/0.5%H_2O) upon the stepwise addition of $[Bu_4N]^+[H_2PO_4]^-$ (from top to bottom: 0.0, 0.38, 0.74, 1.07, 1.38, 1.67, 1.94, 2.31, 2.86, 3.33, 3.75, 4.44, 5.00 equivalents).

Job plot and titration curve analysis

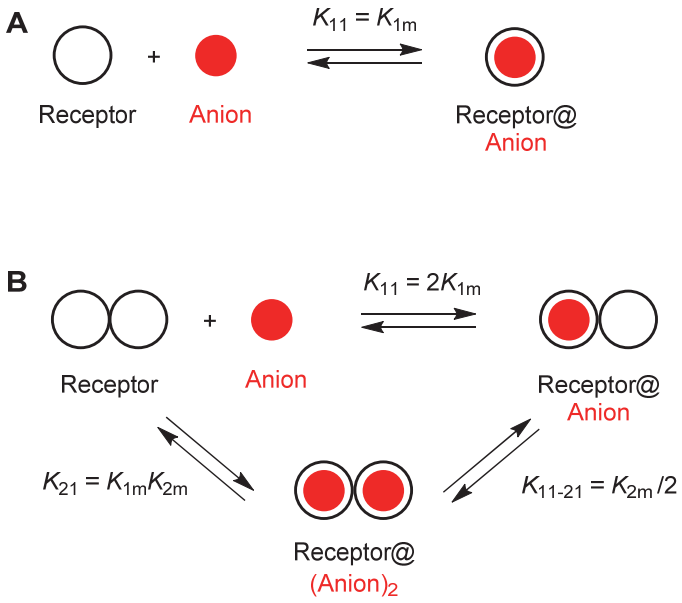

Scheme S1. Schematic representation of the species and equilibria involved in the formation of a 1:1 anion/receptor complex (A) and the stepwise formation of a 2:1 anion/receptor complex (B). The stability constant of the 1:1 complex (K_{11}), 2:1 complex (K_{21}) and the stepwise constant ($K_{11\text{-}21}$) are shown and related to the microscopic binding constants (K_{1m}, K_{2m}). The data were fitted using HypNMR software.[4]

It should be noted that no clear distinction can be made between the ^{1}H NMR signals of the 1:1 and 2:1 complexes throughout the titration. In the data analysis using a 2:1 model, both urea binding sites were therefore treated as equal, i.e. $K_{1m} = K_{2m}$ (cooperativity factor $\alpha = 1$). Furthermore, the data was initially fitted to a 1:1 model to afford K_{11}, after which the stability constant of the 2:1 complex [$K_{21} = (K_{11}/2)^2$] was included.

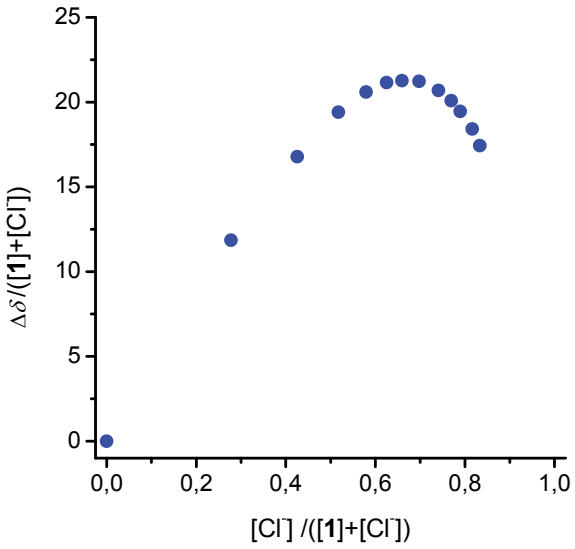

Figure S24. Job plot analysis generated from the addition of $[Bu_4N]^+[Cl]^-$ to (*Z*)-**1** indicating a 2:1 binding stoichiometry.

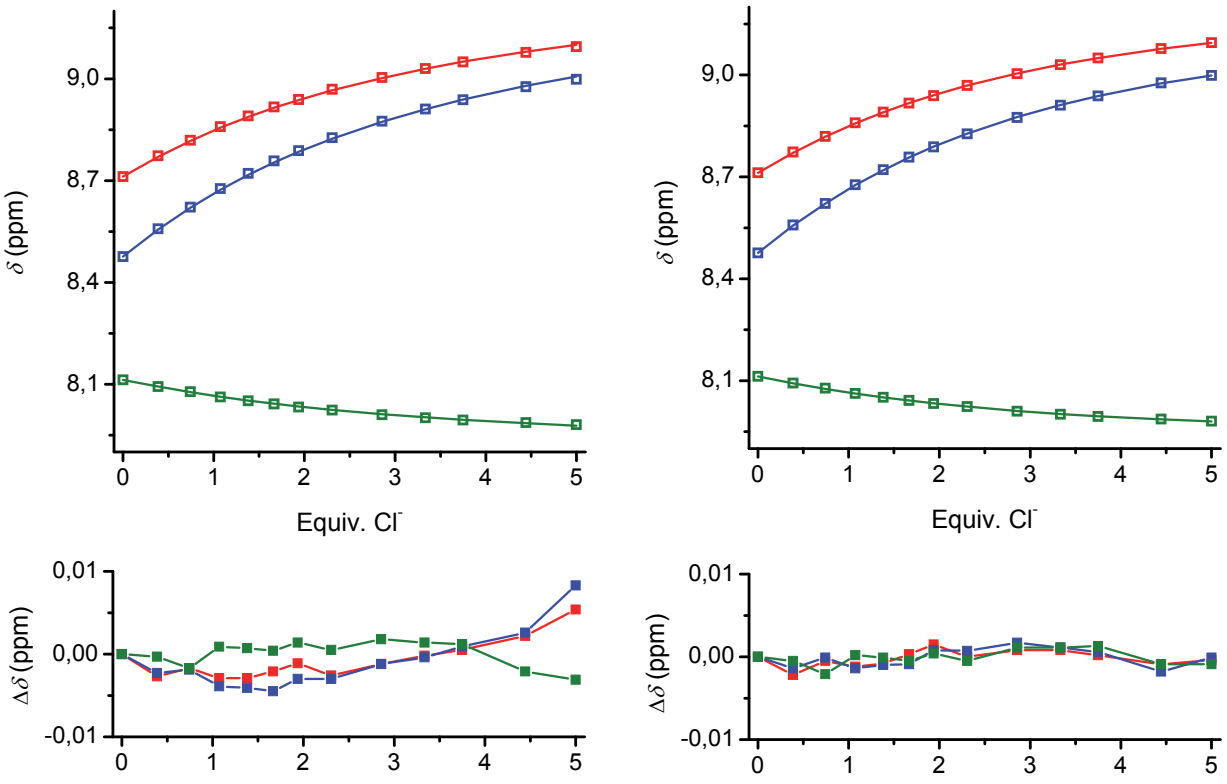

Figure S25. Titration curves for the addition of $[Bu_4N]^+[Cl]^-$ to (*Z*)-**1** and data fitting obtained by simultaneous analysis of the urea-NH (red, blue) and arom-H (green) signals using either a 1:1 (left) or a 2:1 (right) binding model. Based on the residuals analysis, the latter binding model is more likely to be correct: $K_{1m} = 66\ M^{-1}$ (for 1:1); $K_{1m} = 33\ M^{-1}$ (for 2:1).

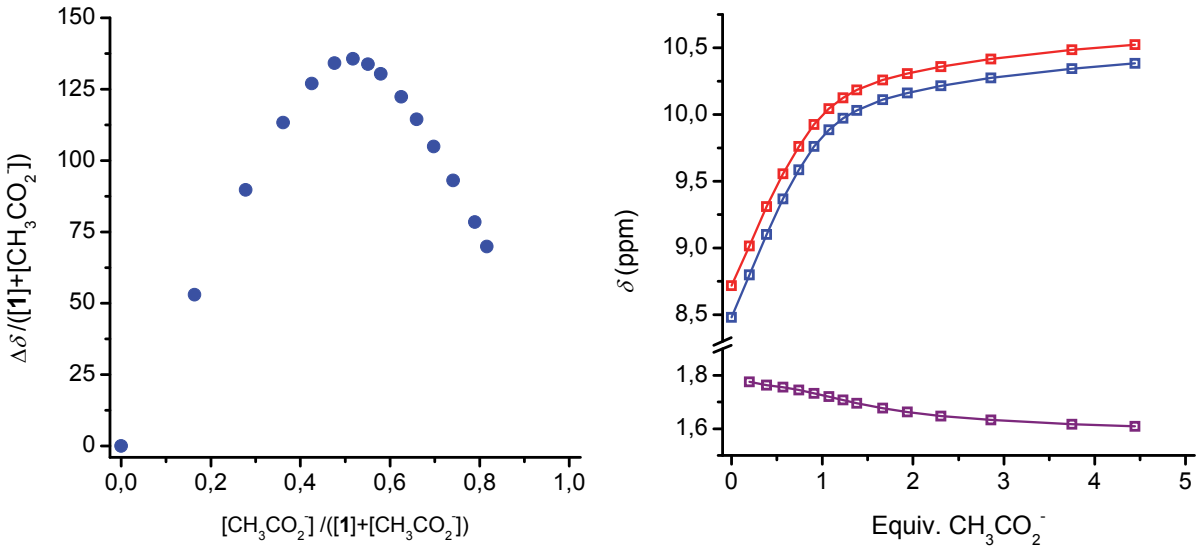

Figure S26. (left) Job plot analysis generated from the addition of $[Bu_4N]^+[CH_3CO_2]^-$ to (*Z*)-**1** indicating 1:1 binding. (right) Titration curves and data fitting to a 1:1 model obtained by analysis of the urea-NH (red, blue) and $CH_3CO_2^-$ (purple) signals: $K_{1m} = 1.40 \times 10^3$ M^{-1}.

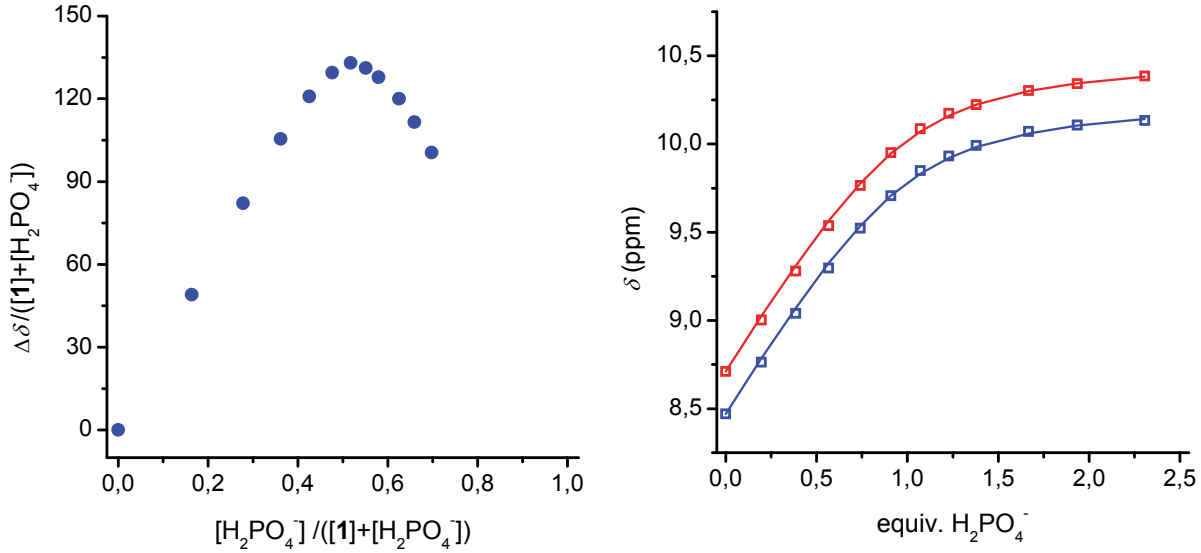

Figure S27. (left) Job plot analysis generated from the addition of $[Bu_4N]^+[H_2PO_4]^-$ to (*Z*)-**1** indicating 1:1 binding. (right) Titration curves and data fitting to a 1:1 model obtained by analysis of the urea-NH (red, blue) signals: $K_{1m} = 2.02 \times 10^3$ M^{-1}.

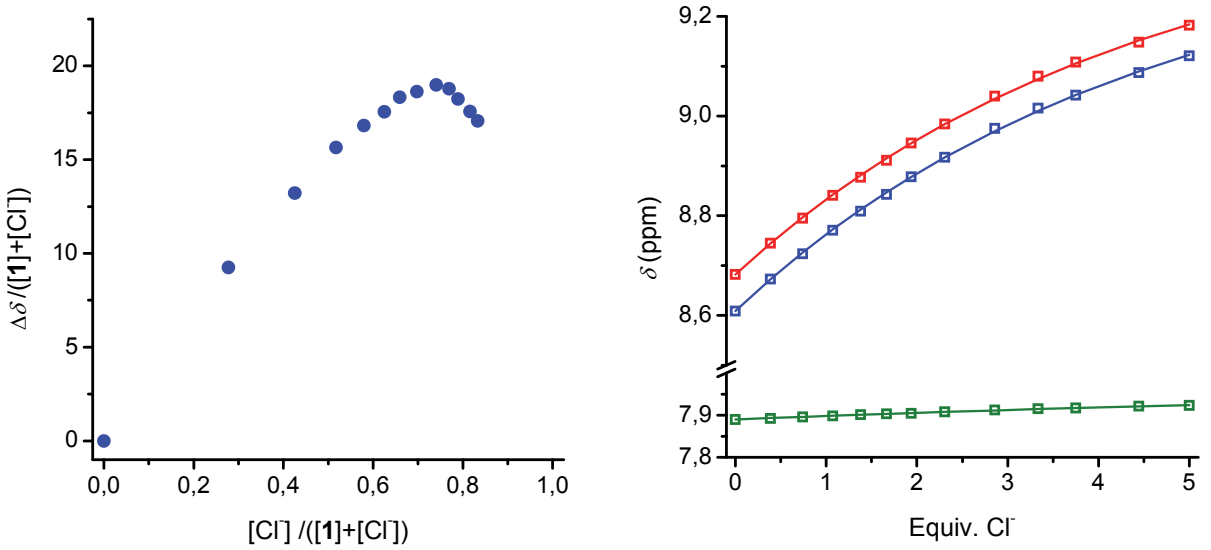

Figure S28. (left) Job plot analysis generated from the addition of $[Bu_4N]^+[Cl]^-$ to (*E*)-**1** indicating 2:1 binding. (right) Titration curves and data fitting to a 2:1 model obtained by simultaneous analysis of the urea-NH (red, blue) and arom-H (green) signals: $K_{1m} = 17\ M^{-1}$.

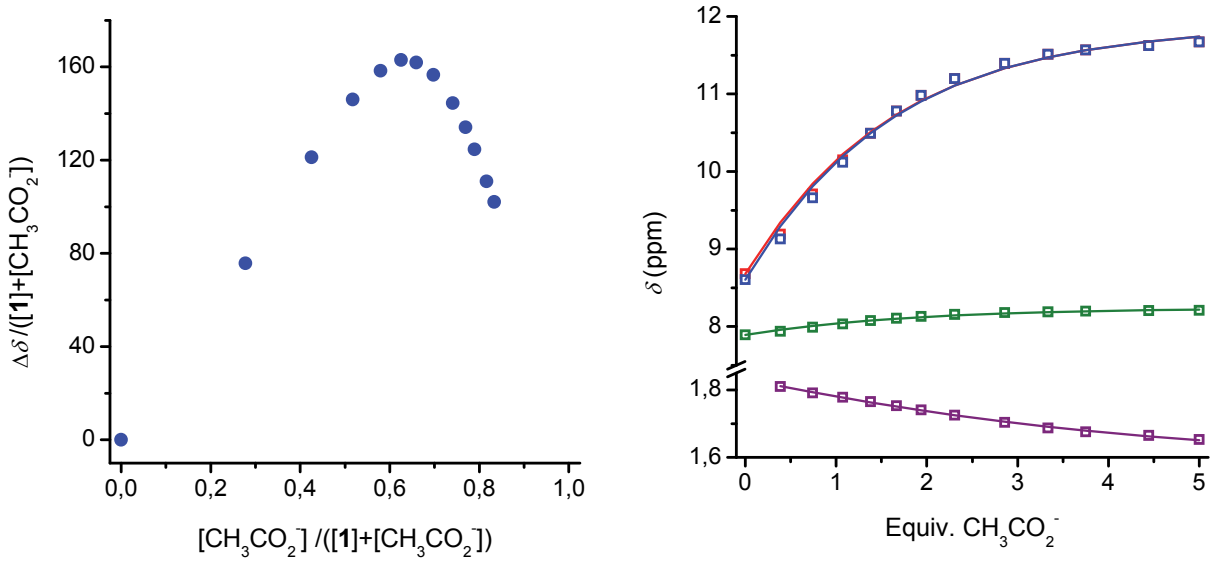

Figure S29. (left) Job plot analysis generated from the addition of $[Bu_4N]^+[\ CH_3CO_2]^-$ to (*E*)-**1** indicating 2:1 binding. (right) Titration curves and data fitting to a 2:1 model obtained by simultaneous analysis of the urea-NH (red, blue), arom-H (green) and $CH_3CO_2^-$ (purple) signals: $K_{1m} = 1.04 \times 10^2\ M^{-1}$.

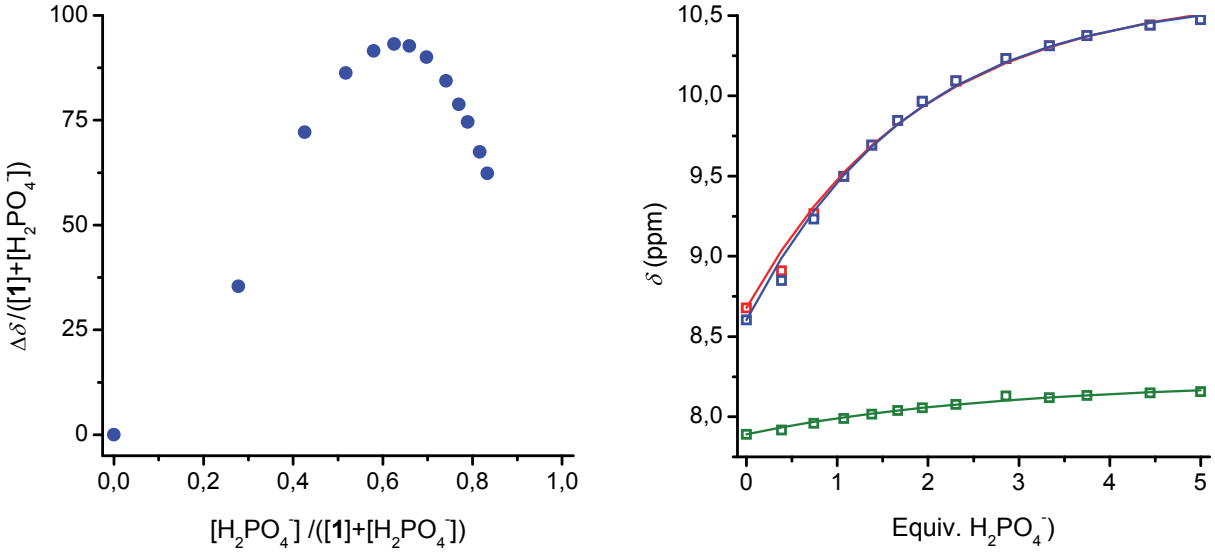

Figure S30. (left) Job plot analysis generated from the addition of $[Bu_4N]^+[\ H_2PO_4]^-$ to (*E*)-**1** indicating 2:1 binding. (right) Titration curves and data fitting to a 2:1 model obtained by simultaneous analysis of the urea-NH (red, blue) and arom-H (green) signals: $K_{1m} = 77\ \text{M}^{-1}$.

Geometry optimizations by DFT

The Gaussian 09 program[5] was used for geometry optimizations and the calculation of energies. Initially, different input geometries were optimized at the semi-empirical PM6 level to find the global minima. Further geometry optimizations were performed at the DFT B3LYP/6-31G++(d,p) level using tight convergence criteria and using an IEFPCM DMSO solvation model. The DFT geometries were found to have zero imaginary frequencies.

Table S1. Cartesian coordinates of (*Z*)-**1**⊃$CH_3CO_2^-$.

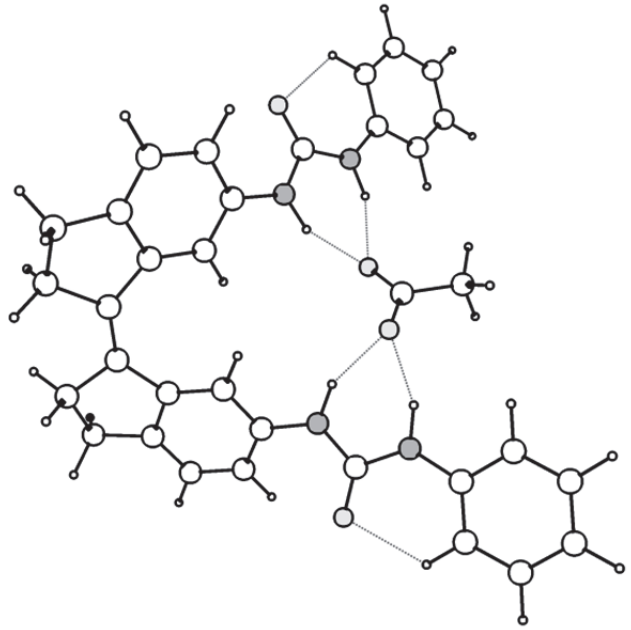

symmetry c1

atom	X	Y	Z
C	-0.481458000	4.584697000	-0.366837000
C	0.655949000	4.563943000	0.375700000
C	1.535310000	3.466975000	0.835860000
C	2.437834000	3.963913000	1.802106000
C	2.170430000	5.421034000	2.092233000
C	1.290556000	5.856855000	0.896109000
C	-1.398904000	3.520589000	-0.830672000
C	-2.272422000	4.049186000	-1.806835000
C	-1.948211000	5.494880000	-2.096196000
C	-1.065768000	5.899493000	-0.891000000
C	1.678336000	2.150322000	0.372767000
C	2.690959000	1.327445000	0.894436000
C	3.552418000	1.820153000	1.891628000
C	3.428096000	3.140789000	2.331618000
C	-1.596919000	2.212073000	-0.365030000

C	-2.635804000	1.426154000	-0.893824000
C	-3.466660000	1.948593000	-1.902286000
C	-3.286951000	3.262186000	-2.344530000
C	-3.980642000	-0.570203000	-0.259365000
O	-5.082295000	-0.108733000	-0.587241000
C	3.956681000	-0.705826000	0.222167000
O	5.082269000	-0.260117000	0.483633000
N	-2.787321000	0.111127000	-0.401772000
N	2.786626000	0.003807000	0.410042000
N	-3.801795000	-1.823413000	0.294716000
N	3.724333000	-1.965933000	-0.295163000
C	-7.028583000	-3.687305000	0.662409000
C	-6.580681000	-4.844605000	1.304653000
C	-5.217391000	-4.968770000	1.597583000
C	-6.145585000	-2.661161000	0.310809000
C	-4.774935000	-2.785717000	0.607084000
C	-4.325010000	-3.954794000	1.255346000
C	4.160718000	-4.104712000	-1.283623000
C	5.015492000	-5.138409000	-1.661321000
C	6.391637000	-5.045902000	-1.421802000
C	4.662041000	-2.948243000	-0.650759000
C	6.045802000	-2.855316000	-0.408938000
C	6.890805000	-3.900211000	-0.796692000
O	0.890480000	-1.919657000	-0.526051000
C	-0.050717000	-2.458176000	0.132527000
O	-0.987570000	-1.814653000	0.698216000
C	-0.082846000	-3.981855000	0.233184000
H	4.323620000	1.178208000	2.296084000
H	-4.258352000	1.336164000	-2.311978000
H	3.087946000	6.010411000	2.186293000
H	1.617454000	5.534243000	3.035087000
H	0.544210000	6.605305000	1.175274000
H	-2.842218000	6.117641000	-2.200922000
H	-1.380950000	5.586297000	-3.032935000
H	-0.291531000	6.622160000	-1.161906000
H	-1.953610000	-0.345833000	-0.017116000
H	1.925795000	-0.436116000	0.069820000
H	1.922392000	6.306886000	0.116596000
H	-1.689670000	6.370045000	-0.117199000
H	1.046854000	1.764704000	-0.419722000
H	4.115743000	3.521125000	3.082943000
H	-0.988233000	1.805936000	0.435111000
H	-3.952156000	3.665791000	-3.103905000
H	-2.834674000	-2.067920000	0.532857000
H	2.740476000	-2.198423000	-0.467971000
H	-8.083035000	-3.572654000	0.425738000
H	-7.276861000	-5.633656000	1.571941000
H	-4.843502000	-5.858423000	2.096617000
H	-6.504512000	-1.770914000	-0.184989000
H	-3.269496000	-4.060987000	1.489933000

H	3.095107000	-4.185137000	-1.479987000
H	4.602148000	-6.017844000	-2.147122000
H	7.058591000	-5.850074000	-1.717071000
H	6.444144000	-1.974464000	0.073435000
H	7.956090000	-3.810044000	-0.601678000
H	0.893472000	-4.419920000	0.016601000
H	-0.802482000	-4.368311000	-0.498356000
H	-0.420179000	-4.296487000	1.224253000

Sum of electronic and zero-point Energies= –1834.007803

Table S2. Cartesian coordinates of (*Z*)-**1**⊃$H_2PO_4^-$.

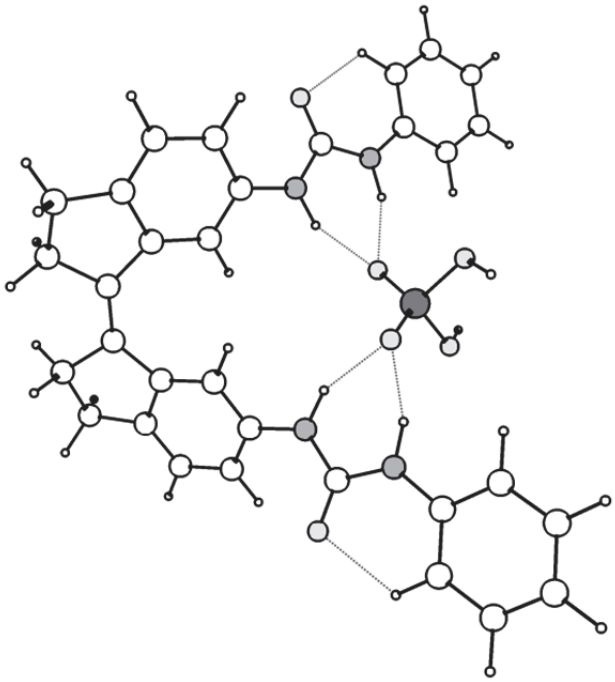

symmetry c1

---

atom	X	Y	Z
C	0.591779000	4.700275000	0.390979000
C	-0.531371000	4.709178000	-0.372753000
C	-1.432631000	3.638013000	-0.852481000
C	-2.289913000	4.160919000	-1.846146000
C	-1.964727000	5.606502000	-2.134011000
C	-1.118351000	6.019103000	-0.906215000
C	1.485163000	3.616257000	0.855623000
C	2.358853000	4.122748000	1.843423000
C	2.050804000	5.568818000	2.147079000
C	1.193185000	6.000014000	0.933629000
C	-1.638667000	2.332642000	-0.380430000
C	-2.676594000	1.548569000	-0.914719000

C	-3.487878000	2.063726000	-1.942626000
C	-3.296063000	3.371697000	-2.395321000
C	1.670844000	2.311439000	0.373713000
C	2.705190000	1.512589000	0.891884000
C	3.535719000	2.012670000	1.911640000
C	3.363777000	3.319653000	2.374875000
C	4.057638000	-0.468721000	0.221345000
O	5.159673000	-0.000232000	0.535619000
C	-4.062911000	-0.420927000	-0.277591000
O	-5.150814000	0.050675000	-0.633548000
N	2.861053000	0.205852000	0.378398000
N	-2.856341000	0.242845000	-0.406759000
N	3.876760000	-1.721751000	-0.329575000
N	-3.909706000	-1.667127000	0.296264000
C	7.107456000	-3.553908000	-0.800968000
C	6.647637000	-4.724579000	-1.409712000
C	5.275219000	-4.868402000	-1.645566000
C	6.227164000	-2.533382000	-0.427001000
C	4.847416000	-2.678457000	-0.665157000
C	4.385164000	-3.860747000	-1.279659000
C	-4.467748000	-3.786550000	1.262371000
C	-5.377197000	-4.783732000	1.608751000
C	-6.737950000	-4.638373000	1.313677000
C	-4.898312000	-2.613438000	0.608500000
C	-6.266265000	-2.466923000	0.310629000
C	-7.166326000	-3.476936000	0.665598000
H	-4.276639000	1.451225000	-2.357494000
H	4.322199000	1.388441000	2.313672000
H	-2.858289000	6.224493000	-2.266498000
H	-1.371132000	5.696553000	-3.054456000
H	-0.346668000	6.752222000	-1.155202000
H	2.951670000	6.177394000	2.273585000
H	1.469907000	5.656276000	3.075819000
H	0.428716000	6.734798000	1.199577000
H	2.032180000	-0.251280000	-0.006764000
H	-2.044320000	-0.214870000	0.012028000
H	-1.768283000	6.478744000	-0.147384000
H	1.837058000	6.464684000	0.172743000
H	-1.039997000	1.931658000	0.430542000
H	-3.947737000	3.770315000	-3.168873000
H	1.058308000	1.921590000	-0.432225000
H	4.028779000	3.706407000	3.143082000
H	2.905543000	-1.974482000	-0.535637000
H	-2.948765000	-1.921157000	0.545258000
H	8.169211000	-3.424010000	-0.609161000
H	7.341833000	-5.509031000	-1.695068000
H	4.892359000	-5.768846000	-2.117681000
H	6.594842000	-1.632848000	0.043228000
H	3.322157000	-3.982050000	-1.469346000
H	-3.414098000	-3.909099000	1.497742000

H	-5.018677000	-5.677259000	2.112093000
H	-7.447250000	-5.414668000	1.583799000
H	-6.609698000	-1.573258000	-0.190035000
H	-8.218548000	-3.346085000	0.427468000
O	-1.106332000	-1.741208000	0.803339000
P	-0.012590000	-2.511065000	0.089308000
O	1.048264000	-1.785486000	-0.715119000
O	-0.788336000	-3.598306000	-0.865364000
O	0.807886000	-3.439292000	1.166686000
H	-0.183976000	-4.026736000	-1.490439000
H	0.222453000	-3.809524000	1.844659000

Sum of electronic and zero-point Energies= –2249.117127

References

(1) Feldmeier, C.; Bartling, H.; Riedle, E. Gschwind, R. M. *J. Magn. Reson.* **2013**, *232*, 39-44.

(2) Montalti, M.; Credi, A.; Prodi, L.; Gandolfi, M. T. *Handbook of Photochemistry, Third Edition*., CRC Press, Boca Raton, Fl, **2006**.

(3) Hatchard, C. G.; Parker, C. A. *Proc. Roy. Soc.* **1956**, *A235*, 518-536.

(4) C. Frassineti, S. Ghelli, P. Gans, A. Sabatini, M. S. Moruzzi and A. Vacca, *Anal. Biochem.* **1995**, *231*, 374-382.

(5) Gaussian 09, Revision D.01, Frisch, M. J.; Trucks, G. W.; Schlegel, H. B.; Scuseria, G. E.; Robb, M. A.; Cheeseman, J. R.; Scalmani, G.; Barone, V.; Mennucci, B.; Petersson, G. A.; Nakatsuji, H.; Caricato, M.; Li, X.; Hratchian, H. P.; Izmaylov, A. F.; Bloino, J.; Zheng, G.; Sonnenberg, J. L.; Hada, M.; Ehara, M.; Toyota, K.; Fukuda, R.; Hasegawa, J.; Ishida, M.; Nakajima, T.; Honda, Y.; Kitao, O.; Nakai, H.; Vreven, T.; Montgomery, J. A., Jr.; Peralta, J. E.; Ogliaro, F.; Bearpark, M.; Heyd, J. J.; Brothers, E.; Kudin, K. N.; Staroverov, Keith, T.; V. N.; Kobayashi, R.; Normand, J.; Raghavachari, K.; Rendell, A.; Burant, J. C.; Iyengar, S. S.; Tomasi, J.; Cossi, M.; Rega, N.; Millam, J. M.; Klene, M.; Knox, J. E.; Cross, J. B.; Bakken, V.; Adamo, C.; Jaramillo, J.; Gomperts, R.; Stratmann, R. E.; Yazyev, O.; Austin, A. J.; Cammi, R.; Pomelli, C.; Ochterski, J. W.; Martin, R. L.; Morokuma, K.; Zakrzewski, V. G.; Voth, G. A.; Salvador, P.; Dannenberg, J. J.; Dapprich, S.; Daniels, A. D.; Farkas, Ö.; Foresman, J. B.; Ortiz, J. V.; Cioslowski, J.; Fox, D. J. Gaussian, Inc., Wallingford CT, **2013**.